Nr 127, 2007

SMHI

Meteorologi

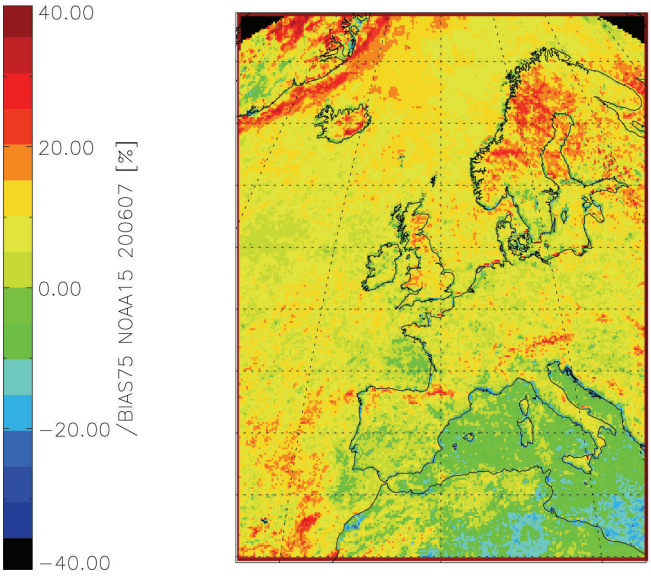

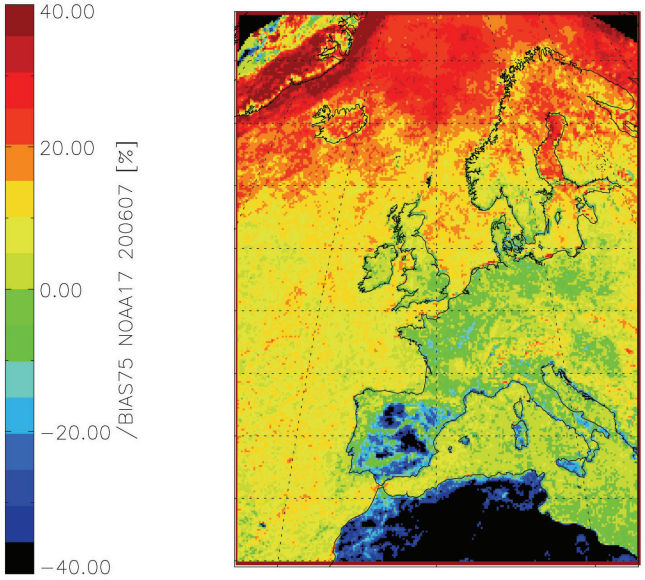

METEOSAT 8 SEVIRI and NOAA AVHRR Cloud Products

A Climate Monitoring SAF Comparison Study

Sheldon Johnston and Karl-Göran Karlsson

Cover Image
The difference between the mean cloudiness for Meteosat 8 SEVIRI cloud mask and NOAA 15 (left) respective 17 (right). The month is July 2006. This difference is taken between the monthly mean for each products based on the amount of NOAA scenes available. The area covers CM-SAF baseline area and lies within the MSG viewing field of view.

Meteorologi
Nr 127, 2007

METEOSAT 8 SEVIRI and NOAA AVHRR Cloud Products

A Climate Monitoring SAF Comparison Study

Sheldon Johnston and Karl-Göran Karlsson

Report Summary / Rapportsammanfattning

Issuing Agency/Utgivare

Swedish Meteorological and Hydrological Institute
S-601 76 NORRKÖPING
Sweden

Report number/Publikation

Meteorologi nr 127

Report date/Utgivningsdatum

Juni 2007

Author (s)/Författare

Sheldon Johnston och Karl-Göran Karlsson

Title (and Subtitle/Titel

METEOSAT 8 SEVIRI and NOAA AVHRR Cloud Products. A Climate Monitoring SAF Comparison Study

Abstract/Sammandrag

The goals of this study are to compare the MSG SEVIRI and PPS AVHRR monthly mean cloud products of the CM-SAF. The study was done in two parts: first comparing the cloud mask products and then comparing the cloud top temperature and height products. This was done over a region from Greenland to eastern Russia and as far south as the Sahara. The study covered four seasonally-representative months. For the cloud mask using PPS version 1.0, the results showed large problems over the Sahara and parts of Spain during the summer months. This was primarily due to the high reflectances in channel 3a and most prominent with NOAA 17.

Much larger differences were found over water than over land surfaces, with the exception of Scandinavia where the differences were comparable to those found over water. The cloud-contaminated values were removed in one plot and this revealed that PPS had a larger number of cloud-contaminated pixels than MSG. This agrees with the concept that MSG reports increased cloudiness at higher viewing angles. This also explains why the differences over Scandinavia were so large and positive in value. The NOAA images at high latitudes have better spatial resolution and reports fewer cloudy and cloud-contaminated pixels than MSG.

Sub-pixel and thin clouds greatly affected how well the two products converged. An attempt to use a weighted factor to adjust the effect of cloud-contaminated pixels on the total cloud cover failed to improve the convergence between the two cloud masks. The effect of the MSG viewing angle and the subsequent effects of reporting more cloudy pixels (or cloud-contaminated pixel – to include thin clouds) could be seen throughout all four months in the form of larger positive differences at latitudes approaching 80 degrees. Significant changes were seen with results from the PPS version 1.1. A significant decrease in the difference over the Sahara was the most discernable change. On the other hand, for NOAA 17, the agreement with MSG during twilight conditions was reduced by almost one half. The comparison of the cloud top temperature and height products revealed that MSG reported more low clouds during the summer months than PPS. This was mostly like due to the presence of convective clouds and the angle at which they are viewed (small cumulus clouds when viewed from nadir has a smaller diameter than when viewed slantwise).

Key words/sök-, nyckelord

CM-SAF, MSG SEVIRI, Cloud product comparison

Supplementary notes/Tillägg	Number of pages/Antal sidor	Language/Språk
	42	Engelska

ISSN and title/ISSN och titel

0283-7730 SMHI Meteorologi

Report available from/Rapporten kan köpas från:

SMHI
S-601 76 NORRKÖPING
Sweden

Table of Content

PPS MSG Comparison

1 Intended readers

This report assumes the reader to have good knowledge of satellite and satellite products within the EUEMTSAT project called Satellite Application Facility (SAF). Distribution will primarily be to the meteorologist within SMHI and the Climate SAF consortium.

2 Introduction

Cloud products are today derived from imagery data from both the NOAA polar satellites and the geostationary MSG satellite for various purposes. However, it is still largely unknown whether they can be considered as comparable in quality or if one of the two products is superior to the other. Since there is often little or no "ground truth" to compare with, it is at least important to understand how the two products mutually differ and how the difference might change depending on changes in e.g. viewing and other conditions. For example, it is can be shown the quality of MSG products is reduced at latitudes approaching 80° (i.e., at very high viewing angles). At such high latitudes, the satellite sees more thin clouds and suffers from parallax errors.

The area common for both MSG and NOAA cloud products in the EUMETSAT Climate Monitoring SAF (CM-SAF) project extends from northern Africa up to about latitude 70° N (CM-SAF Science Plan 2001). Areas at or near the equator were not included as there are no polar CM-SAF cloud products produced for these areas. This report describes results from a comparison study aimed at quantifying the differences in performance between the two different cloud algorithms by comparing the cloud mask and cloud top temperature and height products. A background is given followed by the method used and some discussion about the results. The cloud type was excluded from the study at this point due to time constraints but ought to be included in a future study.

3 Background

The METEOSAT Second Generation (MSG) Spinning Enhanced Visible and InfraRed Imager (SEVIRI) delivers all day images of the weather patterns with a resolution of 3 km. The full disc view allows frequent sampling, every 15 minutes, enabling monitoring of rapidly evolving events. EUMETSAT and the Satellite Application Facilities (SAFs) extract information from the SEVIRI data and turn it into products of particular use to meteorologists and climatologists, such as wind field diagrams, water surface temperature, precipitation estimates and analyses of cloud coverage, cloud height and temperature and other cloud properties. The Polar Operational Environmental Satellite (POES) system offers the advantage of daily global coverage by making nearly polar orbits roughly 14.1 times daily. There are currently about 6 polar weather satellites (5 NOAA and 1 Metop) available for use within the CM-SAF. These provide global coverage daily and the receiving station in Germany archives and processes, on average, about 8-18 passes daily. This number is highly dependent on location as we will see later on. The POES satellites carry the Advanced Very High Resolution Radiometer (AVHRR) and the data received supports a broad range of

environmental monitoring applications including weather analysis and forecasting, and climate research. Data from both satellites are used by the CM-SAF to produce similar products: Cloud mask (CFC), Cloud Type (CT), Cloud Top Temperature and Height (CTT, CTP, CTH), Cloud Phase (CP), Cloud Optical Thickness (COT) and Cloud Water Path (CWP). The NOAA KLMN series of satellites include NOAA15, 16, 17 and 18 but in this study NOAA 16 and 18 were not included. The German weather service (DWD) who is hosting the CM-SAF project excluded NOAA 16 in the operational data stream because this satellite has problems with its scan motor and this creates extensive noise in the data. Furthermore, at the time this study was initiated NOAA 18 was not yet available for operational processing.

The DWD generates cloud products from both satellite types (MSG and NOAA) operationally and all the data used in this study was acquired there. This gave the added advantage of having only one Numerical weather prediction (NWP) model influencing the cloud products from both satellites through the use of some necessary background information. Data from cloud processing software versions denoted MSG V1.2 and PPS 1.0 were used, except for one of the studied months (April 2006) where additional results from the upgraded PPS version 1.1 were also available. The original data set consisted of hourly images from MSG and all the NOAA images received that covered the CM-SAF geographical processing domain during a month.

Polar satellite Cloud products from DWD are produced over sub-areas of the Baseline area, called tiles (see Figure 1). These tiles vary slightly in dimensions and cover a large portion of the northern half of the MSG disk. There are 35 tiles in all but not all were used in this study. Twelve tiles of equal dimensions and which cover both land and water areas were selected (Figure 1). The idea was to use only those tiles in the central portion of the Baseline area where we have sufficiently good NOAA AVHRR coverage since we currently use AVHRR-data from only one AVHRR receiving station (Offenbach).

Since MSG has a higher temporal resolution than NOAA satellites, this study used instantaneous scenes of the NOAA and MSG to recreate the monthly means thus ensuring that the mean of each cloud product was based on the same amount of data. The instantaneous scenes were then paired so that no pair was more than 30 minutes apart from each other. Due to the nature of the NOAA overpasses, some tiles had more paired scenes than others. Furthermore the comparison was done on a 15 km resolution grid. This caused some peculiarities in the results which was best seen in data density plots as sharp lines along the boundaries of the tiles. These discontinuities along the borders of tiles are explained by differences in data coverage (i.e., neighbouring tiles did not have the same number of used NOAA overpasses). This coverage is also influenced by fact that the NOAA scenes are not processed if the coverage per tile is less than 50% (adjustable).

There will naturally exists differences between the two products because of the differences in the satellite data sets and the associated algorithms. MSG has 12 channels while NOAA/METOP has 6 (but only 5 are used simultaneously). One very important channel, the SEVIRI 3.9 μm is always used on MSG and on NOAA-15 while NOAA 17 switches between the 1.6 μm channel and the corresponding AVHRR channel at 3.7 μm. The auxiliary data is also different in some cases, eg., the landuse map. In short, MSG has many advantages and tools over PPS but at some point PPS results will be better due to e.g. higher spatial resolution and better viewing conditions at high latitudes. Here in lies some of the reason for the

differences seen in Figures 4a and 4b. Both satellites had orbital times that were close to each other (both NOAA satellites being in the morning orbit).

4 Cloud Products

The cloud products discussed here, derived from European and U.S. imaging instruments on geostationary and polar-orbiting satellites, were developed by the EUMETSAT Nowcasting SAF project (NWC-SAF) and CM-SAF (CM-SAF Science Plan 2001). All the cloud products were taken from the CM-SAF archive at DWD to ensure that the same Numerical Weather Product (NWP) data, in this case from the GME model (CM-SAF Science Plan 2001), was used in all products. This ensures that any error introduced to the cloud products by the NWP background information would be systematic and would influence both product types similarly.

Cloud information is needed for the computation of many near-surface and surface parameters (e.g. temperature, snow coverage) and serves as input for forecasting the circulation and dynamics of the atmosphere.

The central aim of the Cloud Mask product is to delineate all cloud pixels in a satellite scene with high confidence. In addition, the product provides information on the presence of snow, water ice, dust clouds and volcanic plumes and tells users how these results were achieved. The Cloud Mask product is also used to extract other Nowcasting products such as Cloud Type.

The Cloud Mask product, from both the MSG and polar orbiting satellites, is needed by a majority of SAFs, including the CM-SAF, the Ocean and Sea Ice SAF (OSI-SAF) and the Land Surface Analysis SAF (Land SAF).

The Cloud Top Temperature & Height product contains information on the temperature and air pressure at cloud top as well as the cloud top altitude for all pixels identified as cloudy in a satellite scene. These retrievals can be made for opaque and semi-transparent clouds. This product contributes to the analysis and early warning of thunderstorms for Nowcasting applications. Other applications include the cloud top height assignment for aviation forecast activities. The product may also serve as input to mesoscale models (MESAN).

CM-SAF goal with these cloud products are:

- the monitoring of the climate state and its variability,
- the analysis and diagnosis of climate parameters to identify and understand changes in the climate system,
- input for climate models to study processes in the climate system on a European and/or global scale and for climate prediction,
- validation of simulation models (climate and NWP),

Climate data derived from satellite measurements are understood as an important component in the climate observing system that consists of conventional observations, remote sensing

data and data sets which are created by means of numerical weather prediction models. Satellite derived data provide a high spatial coverage compared to conventional surface networks and especially fill gaps in areas with few data such as oceans or land regions with sparse conventional observations. They also provide information which cannot be measured from the ground, like the outgoing radiation at the top of the atmosphere.

Clouds and radiation, before longer term studies of changes in weather conditions and climate can be performed; observations are needed to show the natural variability of the quantity of interest. Conventional climatology is based on surface based observations with its low resolution in space. The inclusion of satellite data in climatological studies is an improvement as it provides high temporal and spatial measurements – depending on satellite data used. This permits studies over a large area, taking into account regional differences.

In this study, we are not specifically comparing results from the additional cloud physical products (Cloud Phase, Cloud Optical Thickness and Cloud Water Path) of the CM-SAF. Such a comparison might be considered later in the future.

By comparing the two different versions of cloud products (SEVIRI- or AVHRR-retrieved), we will, unavoidably, also compare results from two different cloud algorithms. The outline of the study is as follows:

- The cloud products that will be compared are Cloud Fractional Cover (CFC) and Cloud Top Temperature and Height (CTT, CTH).

- As a side issue, performance differences related to the characteristics of underlying surfaces (i.e., land, water or coastal) will also be studied.

- A dataset of four months, where each month will represent a season, will be used.

- The tiles chosen will be spread out over land and sea surfaces, and will take into account latitudinal and longitudinal differences affecting the MSG viewing geometry.

4.1 MSG Cloud Fractional Cover – CFC

The cloud mask retrieval algorithm is based a multi-spectral threshold technique where thresholds are scene-dependent and dynamically adjusted (Derrien and LeGléau, 2005). The thresholds are based on pre-calculated radiative transfer simulations stored in look-up tables. Essential further input parameters are actual geographical data (e.g. land use, topography, etc.) and Numerical Weather Prediction (NWP) analyses. The latter are taken from the DWD GME model (see Majewski et al., 2002) with a temporal resolution of 3 hours and a spatial resolution of about 40 km. There are 40 atmospheric layers between ground and the topmost layer at 0.1 hPa.

4.2 MSG Cloud Top Height and Temperature - CTX

The CTX product contains information on the cloud top pressure, temperature and height for all pixels identified as cloudy in the satellite scene. A first step is to simulate SEVIRI radiances and brightness temperatures in channels 6.2 μm, 7.3 μm, 13.4 μm, 10.8 μm, and 12.0 μm for clear and cloudy scenes using actual NWP temperature and humidity profiles

which were interpolated in time. In order to reduce the computational effort, this is done for boxes of 32 × 32 SEVIRI pixels using the closest NWP grid column values in space. For very low, low, and medium to high thick clouds the cloud-top pressure is then retrieved at pixel resolution and corresponds to the best fit between the simulated and the measured 10.8 μm brightness temperatures. High and semi-transparent clouds are treated as described in Schmetz et al. (1993) and Menzel et al. (1982), respectively, if the first correction fails. Cloud-top temperature and height are then retrieved from the known cloud-top pressure and atmospheric profiles from NWP data sets.

4.3 PPS Cloud Fractional Cover – CFC

Except for the recent advances in the SAF development the experience at SMHI of automatic cloud detection and analysis from satellite data stems mainly from the development and operational use of the SCANDIA model, a multi-spectral cloud analysis scheme based on the processing of NOAA AVHRR data. The principles of the SCANDIA model is described by Karlsson (1989) and a more comprehensive description is provided by Karlsson and Liljas (1990) and Karlsson (1996).
SCANDIA is one of several operational AVHRR cloud algorithms that were initially developed in the mid to late 1980s and early 1990s. Some other related schemes of the same era are APOLLO (Saunders and Kriebel, 1988), LUX (Derrien et al., 1993) and CLAVR (Stowe et al., 1991 and Stowe et al., 1999).

4.4 MSG and PPS CFC Output

The main product output consists of quality flags and the following data format:

0	Non-processed	containing no data or corrupted data
1	Cloud-free	no contamination by snow/ice covered surface, no contamination by clouds; but contamination by thin dust/volcanic clouds not checked
2	Cloud contaminated	partly cloudy or semitransparent. May also include dust clouds or volcanic plumes.
3	Cloud filled	opaque clouds completely filling the FOV. May also include thick dust clouds or volcanic plumes.
4	Snow/Ice contaminated	
5	Undefined	has been processed but not classified due to known separability problems

4.5 PPS Cloud Top Temperature and Height – CTTH

Many NMSs of EUMETSAT member states (including SMHI) use still today the uncorrected brightness temperature information from AVHRR IR imagery as a rough estimation of cloud top temperatures. For the optically thick clouds this estimation is in most cases acceptable. However, for pixels containing semi-transparent or fractional clouds (often representing a large fraction of cloudy pixels) this information is definitely misleading,

yielding sometimes to quite a large underestimation of true cloud top heights. The objective of the SAFNWC CTTH product has been to create a retrieval that as far as possible (considering both computational accuracy and CPU efficiency aspects) compensates for the semi-transparency effect and the effect of an absorbing atmosphere between the cloud top and the satellite sensor. It must, however, be remembered that the NOAA/Metop satellite does not provide the most optimal platform for semi-transparency correction and cloud top temperature and height retrieval in general. The derivation of the cloud top height using the instruments on these satellites will naturally be rather indirect requiring a lot of ancillary data like NWP model output. Other more direct techniques exist, e.g. using stereo-scope imagery requiring a setup of two geostationary satellites with overlapping fields of view. The HIRS instrument with its sounding channels provides the possibility for applying the radiance rationing technique as detailed by Menzel et al (1983). This technique applies to single layers of high semi-transparent clouds. The HIRS channels do, however, have rather poor horizontal and vertical resolution. The AVHRR instrument provides window channels which may be used to build up two dimensional histograms according to a technique based on the work of Inoue (1985) and Derrien et al. (1988). This technique is neither particularly direct, but though it is designed for single layers of semi-transparent cirrus it may also work on broken/sub-pixel clouds. For the SAFNWC CTTH we have chosen the latter technique to be applied to AVHRR data. In the future, the radiance rationing technique using HIRS data may be implemented as a possible complement to the AVHRR algorithm.

4.6 PPS CTTH Output

The CTTH produces three parameters for the cloud top, namely the temperature, the height in meters and the height in pressure units. Also the output format is prepared for the generation of a parameter called *c*loudiness thought to give the cloud cover fraction. But this latter parameter is not retrieved with the current algorithm. It may be retrieved if the radiance ratioing method is to be applied in the future. In addition, for each pixel a set of processing flags describe the method applied and provide information on the conditions under which the pixel was processed, and thought to be important for the assessment of the quality of the cloud top estimation. The CTTH algorithm tries to produce an output for every pixel classified as cloudy by the CT. Cloud free pixels and pixels outside the satellite swath become non-processed. In addition there are conditions when the algorithm is unable to provide an unambiguous estimation no-data value will be assigned to the pixel. The cloud top temperature is stored using a linear conversion from 8bit count to temperature:

$$T = gain \times count + intercept \qquad \text{Eq 2}$$

Where the gain is set to 1 K/count and intercept is set to 100 K. A no-data value is set for all missing data (outside swath) or no data (no result due to failed retrieval or corrupt input data). The cloud top height is stored using a linear conversion from 8bit count to height like as done for the temperature. The gain, intercept and no-data value are set to 200 m for the gain and zero for the intercept.

4.7 MSG CTX Output

Seven bits are used for the cloud top height Linear conversion from count to height:

$$CloudHeight = gain \times count_{7bits} + intercept \quad \text{Eq 3}$$

(correspond to heights ranging between Cloud_Height and Cloud_Height + 200m) where gain is equal to 200 m/count and intercept is equal to -2000 m. Where no height is available a value, zero is used.

Eight bits are used for the cloud top temperature Linear conversion from count to temperature:

$$CloudTemperature = gain \times count_{8bits} + intercept \quad \text{Eq 4}$$

(correspond to temperatures ranging between Cloud_Temperature and Cloud_Temperature + 1K). Gain is set to 1 K/count and intercept to 150 K. Zero is also used where no temperature is available.

5 Data and Method

5.1 Study Area

Since MSG has higher temporal resolution, the total amount of NOAA scenes will determine the datasets size. In addition, due to the nature of the NOAA overpasses where some tiles may get only partial coverage, the quality of the dataset is also determined by the availability of NOAA scenes. The cloud products generated from individual scenes were used to create a new monthly mean instead of the daily or monthly means. This ensured that the compared cloud product means were made up of the same number of scenes. The area chosen consists of the following combination of CM-SAF tiles: 05, 0B, 13, 1D, 06, 0C, 14, 1E, 07, 0D, 15, and 1F. Their positions can be seen in Figure 1 below.

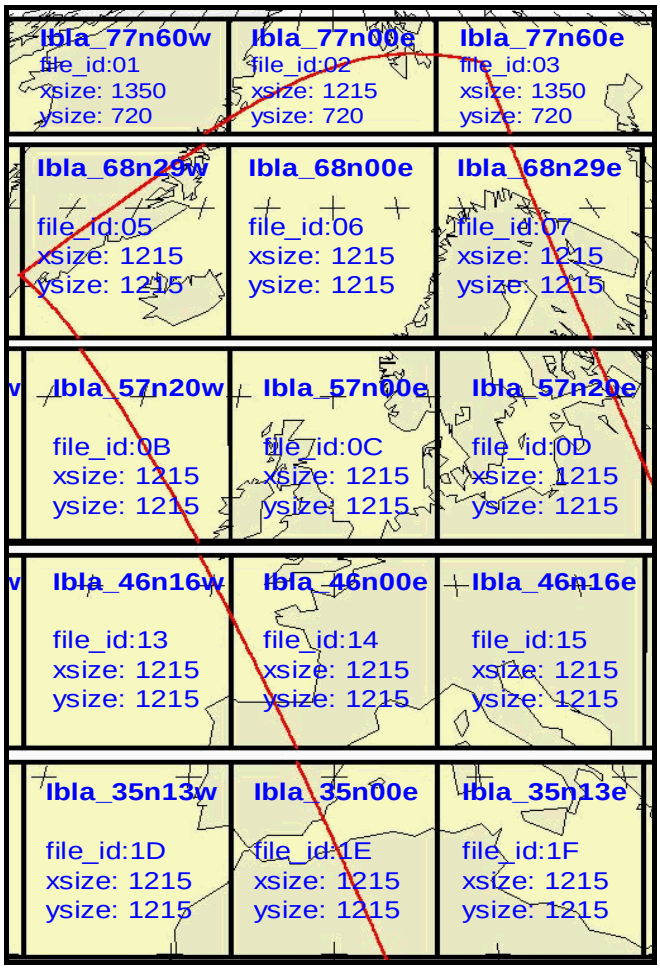

Figure 1: ***CM-SAF tiles used to compare the MSG SEVIRI cloud products with the NOAA PPS cloud products. The red line gives an example of the coverage of one arbitrarily chosen NOAA overpass.***

5.2 Matching the Scenes and Computational Aspects

As a first step, the scenes were paired using date and time. For each NOAA scene, a MSG scene was found that was within ± 30 minutes. This, naturally, reduced the dataset. The MSG cloud products were produced in satellite projection which meant that they had to be reprojected and interpolated onto the corresponding CM-SAF tile (given in sinusoidal projection). Moreover, the nominal resolution of the CM-SAF tiles was 1 km while the resolution of the MSG products varied with latitude. Therefore, there is a considerable oversampling of the MSG products, an oversampling that increases with latitude. The MSG images were taken once an hour at quarter to the hour while the PPS images were less orderly. In general, each tile had anywhere from 50 to 150 paired cloud products per month for the study. The newly adjusted monthly mean was recreated using these paired scenes and only the pixels where both products had valid data. Normally, the monthly mean for both products are available from the CM-SAF product archive but the MSG monthly mean is calculated from many more individual scenes than PPS. Thus, this study reduced significantly the operational MSG dataset required to match the NOAA products. The resulting cloud products were transferred to 15 km resolution before compared. During this transfer, the mean cloud cover was calculated in percentage by extracting, on a pixel by pixel basis, how many fully cloudy pixels and how many partially cloudy pixels there were in each 15 X 15 km grid. This also

allowed for the examination of the effect of the partially cloudy pixels on the total cloud cover.

5.3 Cloud Mask

For each grid point, the mean cloud cover was calculated for the month while keeping track of the number of pixels with valid data within the 15x15 km grid square. The total MSG-PPS difference in cloud cover expressed in percentage was thus calculated using the following equation:

$$CC = \left(\frac{\left(N_{MSG_{cloudy}} + N_{MSG_{partially\_cloudy}} * FC\right) - \left(N_{PPS_{cloudy}} + N_{PPS_{partially\_cloudy}} * FC\right)}{N_{Vp}} \right) * 100 \qquad (1)$$

where Nvp is the number of the valid pixels and FC is the weighting factor for partially cloudy pixels. We will test the impact of changing the value of FC from 0 (if considering partially cloudy pixels as cloud free) to 0.75 and to 1.0 (the latter value considering these pixels as being fully cloudy).

The resulting array was plotted to reveal how the two cloud masks differed from location to location. Several other factors were gleaned from the dataset: the difference in the two cloud products was plotted as a function of MSG's viewing angle, the data density across the entire area, the sunlight conditions, and the coastal effects, to list the major ones.
The Cloud mask products report for each pixel one of 6 possible values: 0, 1, 2, 3, 4, 5.. The values 0, 5 were replaced with the value 255 since no valid data was reported for that pixel. Values 1 and 4 were combined and given the value 1 for clear, leaving 2 (cloud contaminated) and 3 (cloudy filled) to be compared and counted (Eq. 1).

As mentioned earlier, the monthly mean difference was calculated using the same amount of scenes and with scenes that are within 30 minutes of each other. The average time difference between each scene, for the 4 months, is about 15 minutes. Three mean differences were calculated in order to examine both how the two products differed and how the cloud contaminated pixels affected the total cloud cover. It is worth noting that the cloud mask value 2 (the cloud contaminated category) contains all thin clouds detected and these may very well still represent completely overcast pixels. During a previous validation study of MSG cloud mask results against ground-based observation (ORR3 CM-SAF **SAF/CM/DWD/KNMI/SMHI/SR/CLOUDS-ORR/3**,2007) a tuning factor was applied to the fractional cloud category in an attempt to minimize the divergence between the surface observations and MSG cloud mask. This method was again used here in order to evaluate possible changes of results when applying it simultaneously to both MSG and NOAA results. Therefore, the total cloud cover was calculated using the three alternatives for the weighting factor (FC) 100%, 75%, and 0% in Eq. 1.

5.4 Cloud Top Temperature and Height

The comparison was also extended to the CTTH product. The method is given earlier. Beginning with matched scenes that were no more than 30 minutes apart, the MSG products were again re-projected onto the CM-SAF tiles. Only pixels that were valid for both products at the same time were compared. Several things were looked at: how the cloud top height of MSG varied with viewing angle, how the heights and cloud top temperatures were distributed

within the maximum and minimum values, and what is the difference in the mean temperatures and heights for each range.

The method used to compare the CTTH product is an extension of the Cloud Mask method. As mentioned earlier, the cloud top pressure was excluded as it is more abstract than the cloud top height but gives basically the same results. Taking the already paired scenes, the monthly mean was created for both MSG and PPS. Then the difference was taken for each paired pixel with valid data. The data also had a resolution of 15 km. For the temperature, the data was separated into 5K bins and keeping track of the frequency per bin and the average temperature for that interval. Similarly for the height data, it was also separated in this manner. What was then plotted were histograms for the two satellites also with a difference plotted created by taking the difference between the mean values of each satellites for each interval. The CTH was done in a similar manner but the bin interval was set to 500 meters. The average cloud height per bin was calculated. The average heights were calculated as a function of viewing angle.

6 Results and Discussion

6.1 Data Density

There were about 300 polar overpasses per satellite in one month. However, due to the nature of polar orbiting satellites some area had a greater data density than others. No pixel had more than 170 valid measurements per month. Figure 2 shows a plot of the number of overpasses with maximum temporal coverage over the Norwegian Sea.

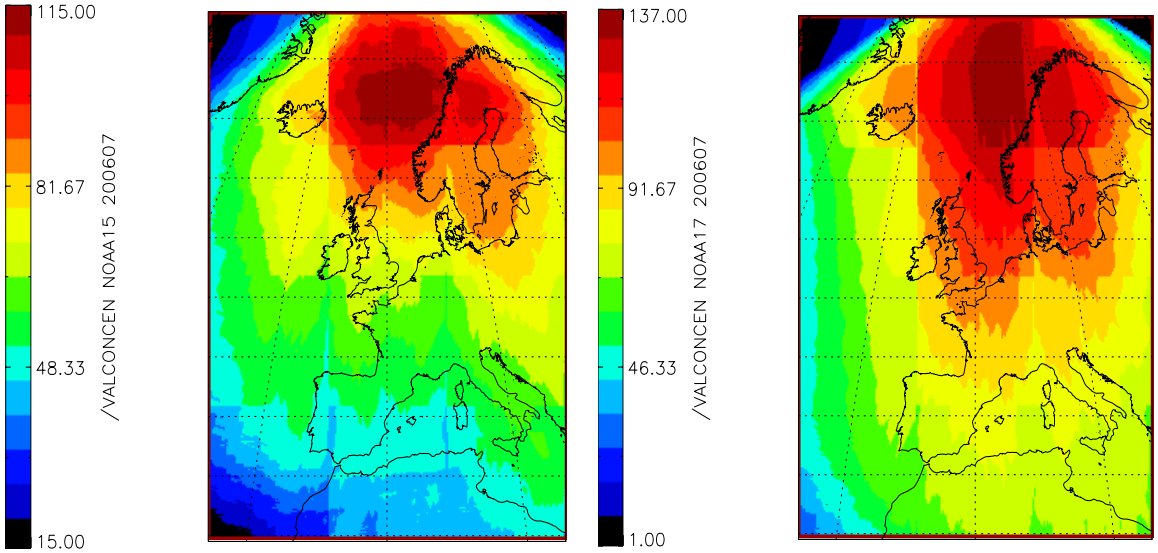

Figure 2: The density of satellite scenes over a one-month period. The colours represent the number of overpasses used at each pixel location. On the left: NOAA15 and on the right: NOAA17. July 2006. The colour bar shows the number of paired cloud products with valid pixels.

The figure shows the data distribution and is representative for all the months studied. The colour bar shows the amount of times a paired pixel had valid data for the month in question. The variation in the number of total scenes per tile gave rise to sharp edges along the image boundaries as explained earlier in the report.

The corresponding frequency plots for the other three months show a similar pattern and were excluded from this report. As expected, the region with the greatest data density is the Norwegian Sea and Northern Scandinavia. The density varies quite a lot between NOAA 15 and 17 with NOAA 17 having the greater amount with up to149 passes. This is due to scheduling conflicts or data loss during retrieval. This low data density is not valid for MSG which has more than 700 images per month (if counting with an hourly time resolution as used in the CM-SAF). Thus, only about 20 % of all MSG scenes were used in this comparison study. As we approached the lower latitudes the NOAA data density drops dramatically. Since PPS is mainly run in the CM-SAF area that does not include the tropic. Later studies could very well include the tropics.

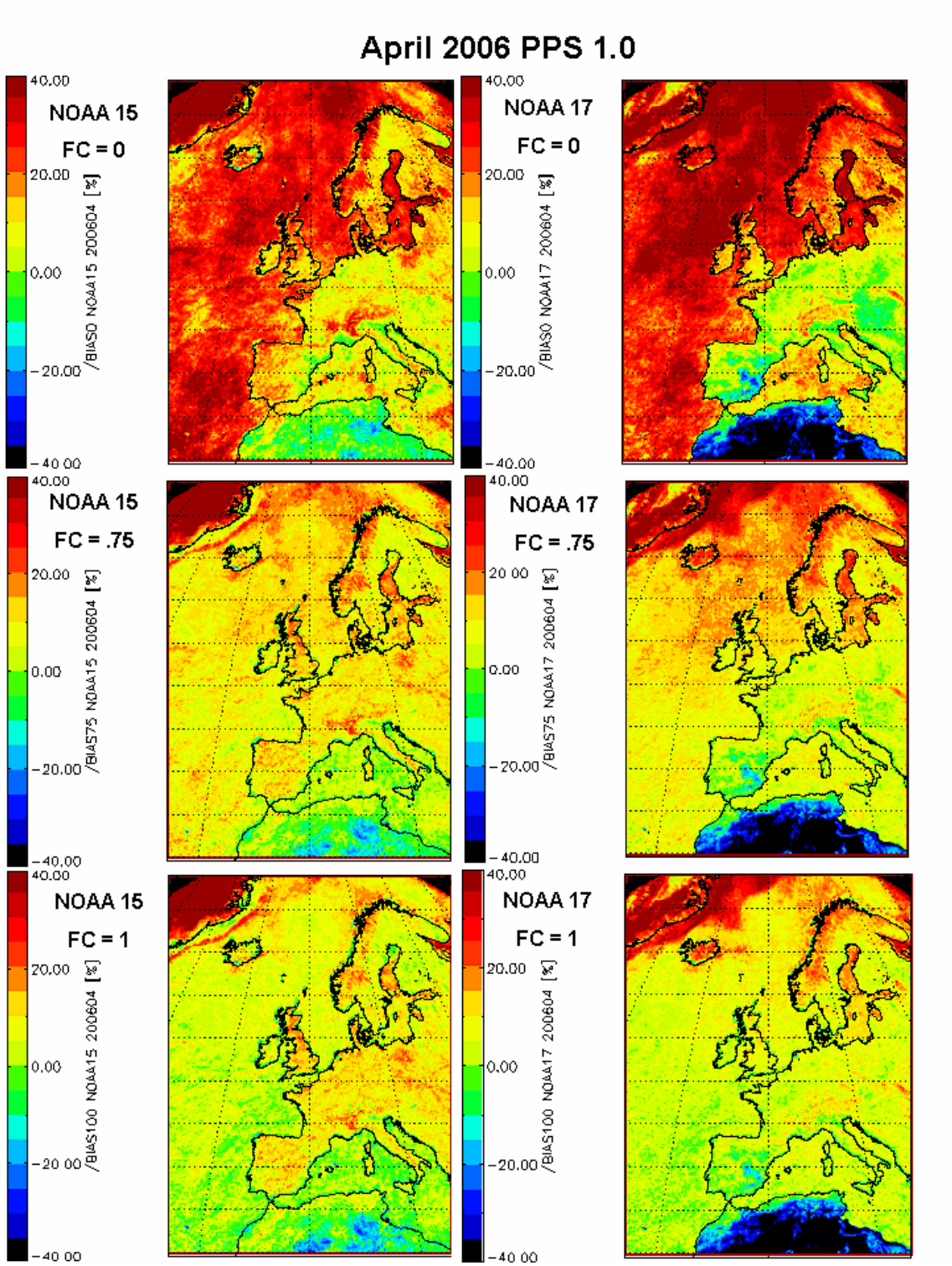

Figure 4a: ***The CFC mean difference MSG cloudiness minus the PPS cloudiness. The cloudiness is expressed in percent. A weighting factor for sub-pixel clouds set to 0 (top), 0.75, (middle) and 1 (bottom). April 2006. On the left are NOAA 15 results and on the right NOAA 17 results.***

6.2 The geographical distribution of Monthly Mean Difference

Figure 4a above shows the differences between the two satellites (MSG respective NOAA 15/17) for April 2006. Results from the other three months are given in Appendix A. Since the study began, some changes were made to the PPS algorithm that targeted some weaknesses experienced over the desert regions, among other things. The effect of these changes results are also given in Figure 4b for the new version PPS 1.1. Unfortunately, only one of the months chosen – April 2006 – was reprocessed using this upgraded algorithm.

6.3 General Features

The main portion of the study looked at the difference between the two satellites across the entire area without separating night and day scenes. The results for the PPS 1.0 version shown in figure 4a revealed much larger differences over sea surfaces than over land for the case ignoring cloud-contaminated pixels (FC=0), top panels) We conclude that since these large differences largely disappears for the case FC=1 we have a much larger number of cloud-contaminated pixels than cloud-filled pixels in the PPS products. Consequently, for the cloud-filled category the situation is the opposite. Largest differences are found over sea surfaces but also over some land portions in the northern part.

The other months showed a similar behaviour between NOAA 15 and 17 and between the NOAA satellites and MSG. However, during December the differences were larger, in particular over land surfaces in Northern Europe

6.4 *The PPS performance over desert surfaces and the impact of a new PPS version*

A large negative difference is seen in Figure 4a over the Sahara desert that is most prominent in the NOAA 17 results. This problem was related to the fact that desert surfaces have a very high reflectance in AVHRR channel 3a (at 1.6 micron) which is comparable to the corresponding reflectance of clouds in this channel. Thus this problem shows up more often in the NOAA 17 images since it uses the 1.6 μm channel during daytime. This is also true for the other four months in the dataset. NOAA 15 also had this problem (surface reflectances are high also in the 3.7 μm channel) but to a far less extent and mostly during October and December 2005. Since PPS 1.0 overestimates cloud cover over the desert, this problem was slightly less when no cloud contaminated pixels were used (FC=0, top panels). All four months showed similar results with July seeing this area even extending to large portions of the Iberian Peninsula.

This problem has been investigated further leading to some changes being made to the PPS algorithm (A.Tetzlaff, 2004). The first version of PPS (version 1.0, used in Figure 4a) was developed and tuned for central and northern European conditions where land surface reflectances in channel 3a normally are much lower than those of clouds. The goal was now to improve the performance of PPS over desert and non-vegetated areas. The problem arose from misclassification of clear sandy areas as cloudy. Emphasis was placed on NOAA 17 images and the channel 3A (1.6μm). In a nutshell, the high spectral reflectivity (0.6μm and 1.6μm) of sandy and non-vegetated areas caused cloud tests to fail in the PPS algorithm. Another cause lies in the use of static thresholds and limits within the USGS landuse maps that did not reflect seasonal changes in the land useage. Also, at night, some minor changes

were made to the threshold tables but the major changes were made during the day. Most of the changes were made to the NOAA 17 algorithm and some alterations were made to the NOAA 15 thermal thresholds over the desert. In addition, the landuse definition for desert barren and shrubland_grassland were redefined and classed as desert when below 45N.

The results given in Figure 4b were processed using PPS version 1.1. Only April 2006 was reprocessed for this study. Adjustments to the PPS algorithm gave significantly reduced differences over the Sahara desert. The results show a marked improvement over the Sahara desert and to a lesser degree, over Spain.

Also other features than the difference over desert surfaces changed when introducing the new PPS version. We notice that the magnitude of the large positive difference over sea surfaces has increased further, especially in the northern part of the area. Over land surfaces differences have instead decreased slightly. Over Greenland, some major shifts occurred and where there was previously a positive difference of about 40%, with PPS 1.1, the results shifted into a deficit being partly below -30%. NOAA 15 results showed greater and more extensive shifts than NOAA 17. Thus, it is obvious that the revised PPS 1.1 algorithm here produces more clouds than the MSG SEVIRI algorithm which is completely the opposite compared to results for PPS 1.0. However, some areas actually converged towards MSG results. These areas were in particular coastal regions.

6.5 *The Influence of The Chosen Weighting Factor for Fractional Clouds*

Since we know about some fundamental differences between the AVHRR and SEVIRI sensors (most important in this respect is perhaps the difference in scanning geometry and varying spatial resolution), it is not obvious that we could treat pixels with fractional cloud cover in the same way as we have done in this study. Nevertheless, we notice that when FC is set to 1, effectively making all cloud contaminated pixels fully cloudy, the results show large positive differences in far fewer areas than for the case ignoring cloud contaminated pixels (FC=0). This indicates that there is at least a fairly good agreement between the two algorithms concerning the amount of cloudy (i.e., the sum of cloud-filled and cloud-contaminated) pixels. Exactly how to count the cloud-contaminated pixels is not obvious but the use of the weighting factor 0.75 (previously deduced when comparing SEVIRI cloud results with surface observations) at least does not increase the differences significantly compared to the case FC=1.

Concerning the changes seen when shifting to PPS version 1.1 it is interesting to notice a more pronounced dependence of the differences on the MSG viewing angle in Figure 4b. Differences now gradually increase from being small or negligible in the most southern part to become large and positive (especially over sea surfaces) in the central portion of the area and, finally, to become very large in the northern part of the area. We may conclude that with the new PPS 1.1 version the impact of algorithm differences appears to be significantly reduced compared to in the previous version 1.0. However, we also notice that there are still specific regions showing differences that cannot be assigned specifically to changes in MSG viewing angles. This concerns in particular areas over Greenland, Iceland and some remaining spots in northern Africa and over the Mediterranean area. A remaining general feature is also the tendency for having much larger positive differences over sea surfaces than over land surfaces.

6.6 Remaining Differences Between N15 and N17 Results

Apart from the differences already described, we notice that results based on PPS 1.0 for NOAA 15 during winter and fall (see Appendix A) show negative differences over Greenland icesheet, while corresponding NOAA 17 results consistently show positive differences for all four months. Along the Greenland coast, however, the difference is reduced, especially when the sub-pixel and thin clouds are removed. The cause of these fluctuations is not fully understood. To better understand what is going here, a more detailed study of, perhaps from products consisting of single scenes and not monthly means, should be done. There was not enough time for this in this study.

The difference in results between the cases when FC set to 1 and 0 in Figures 4a and 4b reveals that the contribution in NOAA results from the fractional cloud category is not only significant over sea surfaces but also over Scandinavia, over central Europe. This is true for both PPS versions and for all four months. Even over Scandinavia, the difference change with latitude is not as dramatic as is, e.g., seen when comparing results over land and over the Baltic Sea.

Finally, we can also see from Figures 4a and 4b that there are various features in the result images resembling the presumed extent and edge of the Arctic sea ice. Thus, it is clear that PPS results (while MSG results being predominately fully cloudy) changes drastically between open ice free ocean and ice covered ocean. Whether this reflects a true change in cloudiness (e.g. convective clouds should form more frequently south of the ice edge) or is due to errors in the cloud detection is not possible to conclude here and needs further studies.

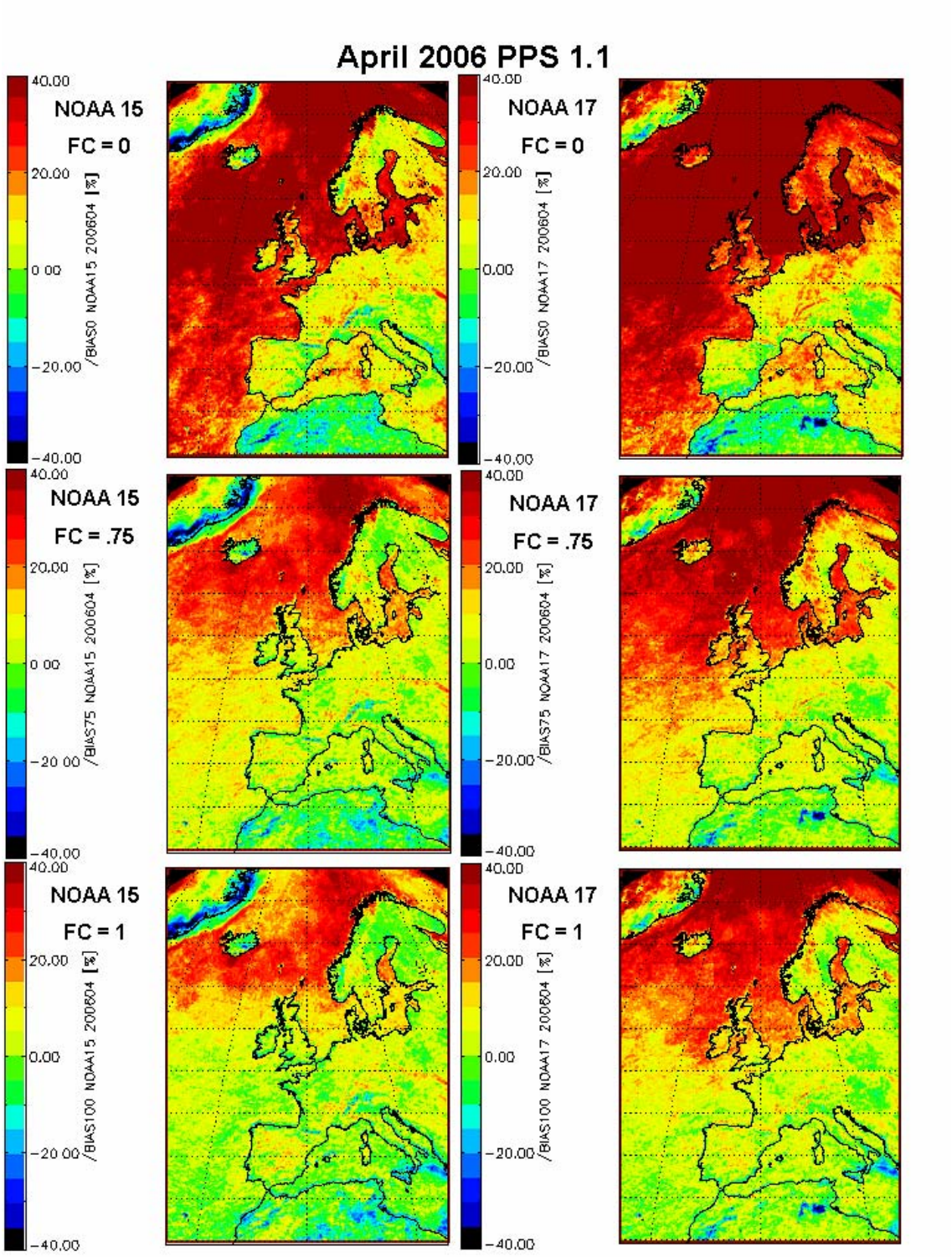

Figure 4b: This figure shows the monthly (MSG-NOAA15) mean difference using a weighted factor of 0 (top), 0.75 (middle), and 1 (bottom) using PPS 1.1. On the left are NOAA 15 results and on the right NOAA 17 results. The month was April 2006.

6.7 Monthly Difference as Function of MSG Viewing Angle

It was considered important to see how the monthly mean cloud amount behaved between these different satellites with changing MSG viewing angle. In order to do this, the MSG viewing angle was calculated across the entire area for all compared pair of scenes. The cloud amount difference was then averaged for each viewing angle taken per degree from lowest reported to the highest (30-90 degrees). The number of valid pixels that went into creating the mean difference in the cloud product with 15 km horizontal resolution was also plotted. The results are shown in Figure 5a for PPS version 1.0 and for all four studied months. The mean cloud amount difference chosen for this portion of the study was the one using weighting factor FC set to 1. This meant that all pixels (cloudy and cloud contaminated) contributed to the total cloudiness with each pixel being 100% cloudy. The corresponding results for April 2006 with the new PPS version 1.1 are shown in Figure 5b.

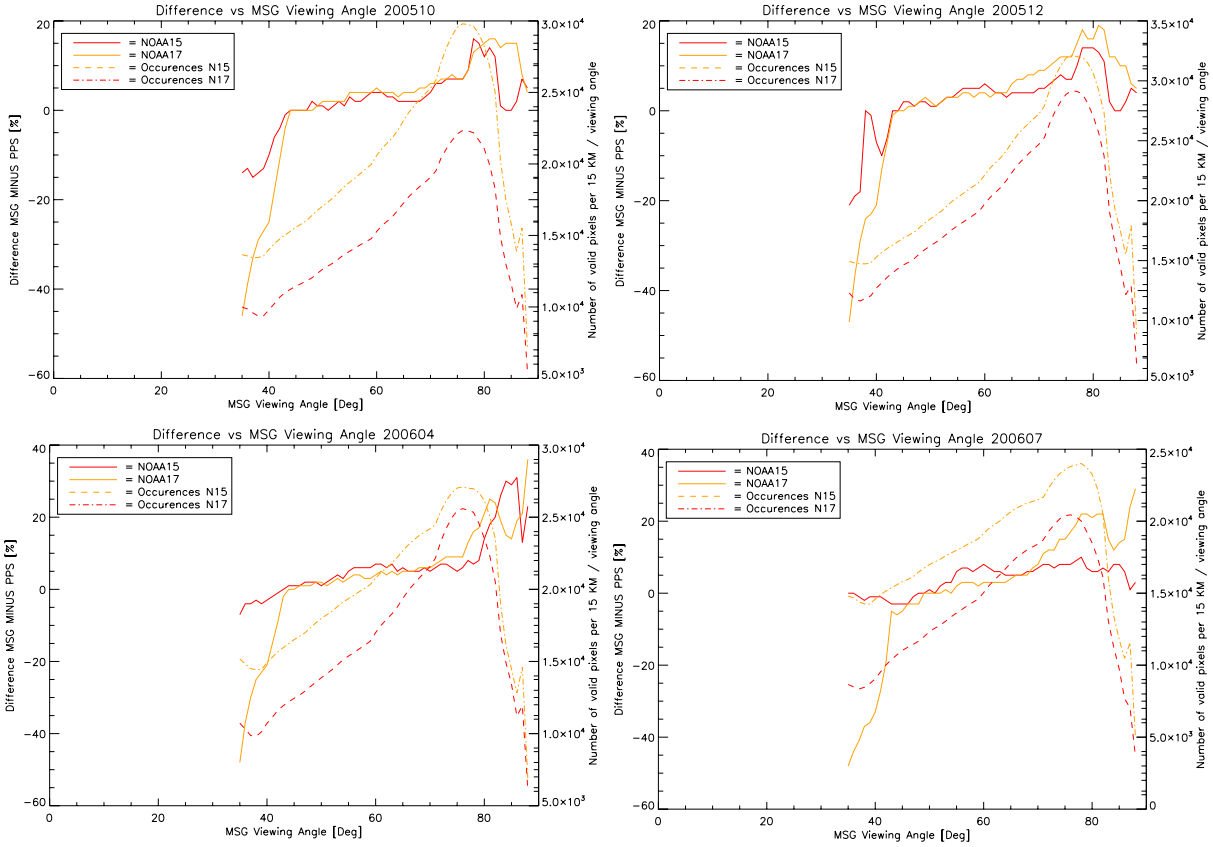

Figure 5a: ***The monthly mean difference as function of MSG viewing angle. All four months are shown here and the PPS version was 1.0. The amount of pixels per satellite (NOAA15 red and NOAA17 yellow) is given by the dashed lines.***

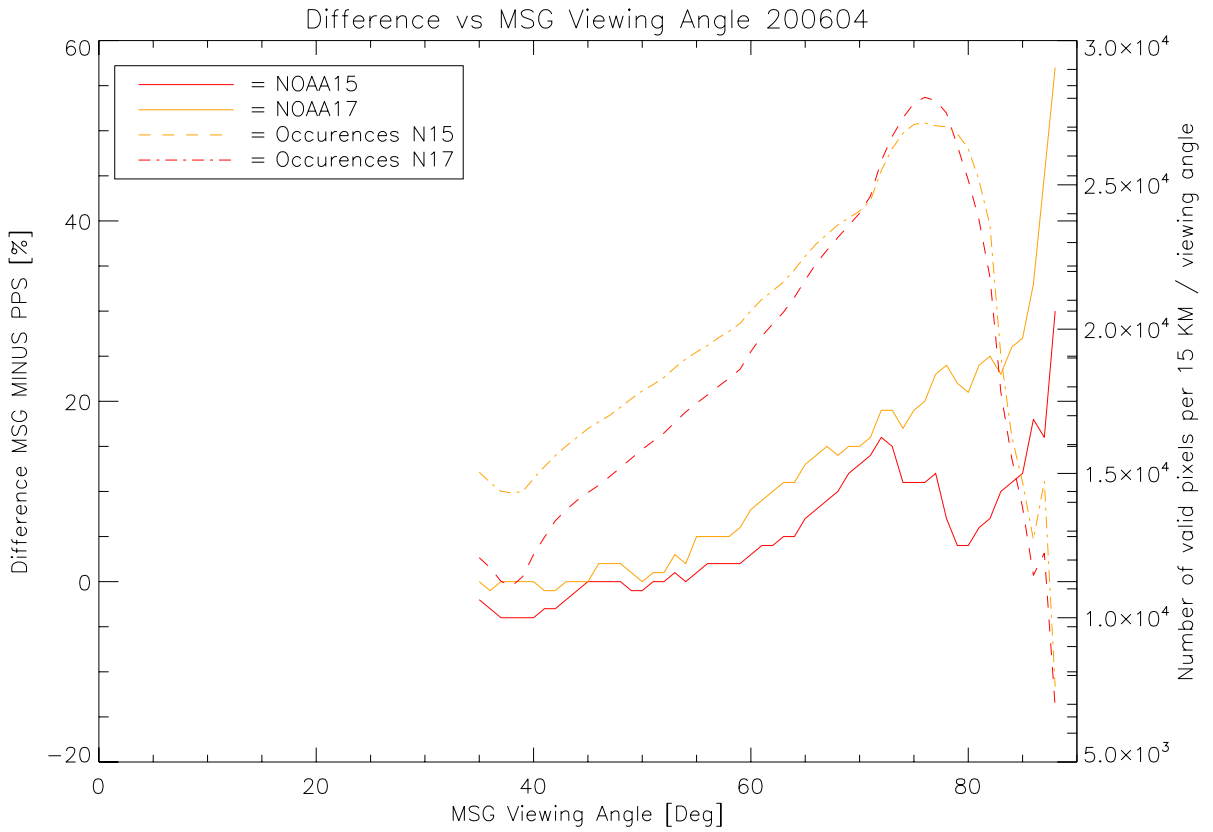

Figure 5b: ***The monthly mean difference as function of MSG viewing angle. April 2006 reprocessed using PPS version 1.1. The amount of pixels per satellite (NOAA15 red and NOAA17 yellow) is given by the dashed lines.***

Since the viewing angle is known to affect the cloud detection ability of any imaging sensor, especially for thin clouds (easier to detect at high viewing angles), this particular behaviour was examined further for the MSG SEVIRI case. Looking at results based on PPS version 1.0 first, Figure 5a shows the cloud amount differences as a function of the MSG viewing angle for the months studied. In addition, the accumulated number of valid pixel values used when calculating the 15x15 km average difference in cloud amount was plotted as a data density plot. As expected, the difference increased for both NOAA satellites with increasing MSG viewing angle. NOAA 17 values had a greater amount of valid data making up each low resolution pixel (i.e., a larger number of NOAA-17 scenes were available – see Figure 2). Both figures show the data density being highest over the Norwegian Sea while also being at a high latitude and a high MSG viewing angle. From 40 up to around 75 degree MSG viewing angle, there is a steady increase in the difference but results for both NOAA satellites remain close to each other. The difference was, on average, only a few percent. Above 75 degrees the difference jumps rapidly to nearly 20 % with NOAA 17 often having the largest values.

Results for the upgraded PPS version 1.1 in Figure 5b (related to results shown in Figure 4b) look much better in this respect. The small changes in the density plot were due to the fact that the reprocessed data did not contain exactly all the original images used in PPS 1.0. PPS 1.1 results showed that NOAA 17 difference was consistently higher than the NOAA 15 difference. The greatest change could be seen in the lowest viewing angles (related to the improvements over desert surfaces) and again near 80 degrees. At these extreme angles, the dataset drops off due to the loss of valid data but the impact of the major changes in PPS 1.1 over the desert is nevertheless well covered at low MSG angles.

At high angles, theory dictates that MSG should report more clouds since thin clouds will look more opaque due to higher optical path-lengths through clouds and they should therefore be more easily detected. Also, clouds with a high vertical extension (e.g. convective clouds) will be projected to cover larger areas than in reality. At third effect lies in the different field of views (FOV) of the two types of satellites. These effects imply that the MSG-PPS difference should increase with increasing MSG viewing angle. In Figure 5b, both satellites now show a steady and monotonous increase (however, with an exception for NOAA15 results near 80 degrees viewing angle) in the difference as the angle approaches 90 degrees. It can also be noted that even if (as previously mentioned) the difference has drastically decreased (even into negative values) over Greenland and at some other places after introducing PPS 1.1, the overall results are still practically the same at very high viewing angles. This means that some compensation has taking place so that additional cloudy PPS pixels have simultaneously appeared over water surfaces with PPS 1.1. This is also clearly seen if comparing e.g. Figures 4a and 4b. One possible explanation of this could be that PPS 1.1 channel 3b scheme tends to classify sea-ice as clouds. In future studies this could be verified by looking at individual scenes.

6.8 Coastal Effects

Another aspect of this study was to examine how the two products agreed in coastal areas. The PPS products from the DWD were not calculated using the in-built coastal scheme so this portion of the study can be seen as a separate test of the need of using it in the future. If we find large differences compared to the results over land and water the use of a coastal specific scheme would be necessary. A fraction-of-land array is always generated when the PPS cloud product is generated. This was used to determine when a pixel was located over a coastal area or not. A coast was defined as any pixel where the fraction-of-land value was between 25 and 75 %. All other pixel values were assigned with no-data values.

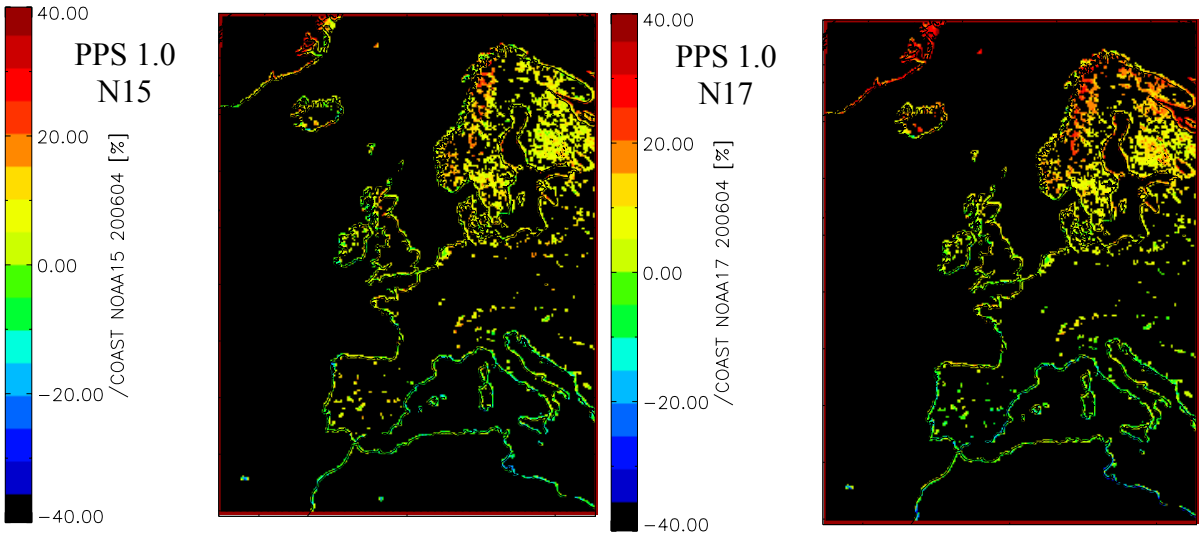

Figure 5a: ***The above images show the adjusted monthly mean difference along coastal regions. The difference is given in percentage and shows from top down and left to right Oct, Apr 2006. The polar satellite used was NOAA15.***

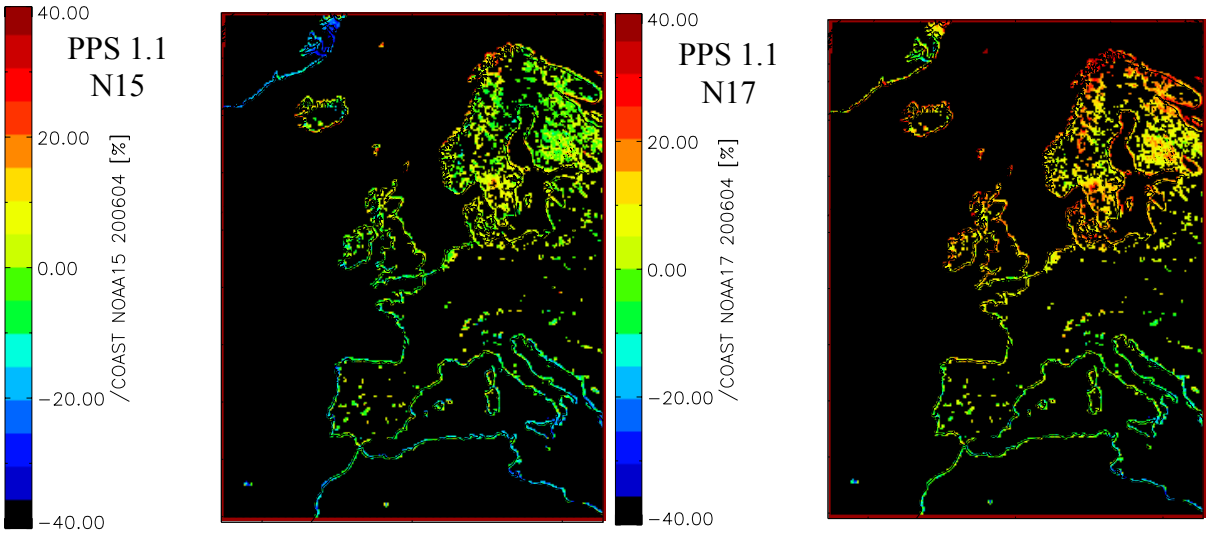

Figure 5b: The MSG-PPS difference in monthly mean cloud amount along coastal regions for April 2006 and for NOAA-15 results based on PPS 1.1.

The effects along coastal areas were examined simply by using a fraction-of-land mask to isolate the coastal areas. The difference was calculated using weighting factor FC set to 1.0. The hope was to be able to look at these regions without interference from the surrounding data. The figures revealed some interesting effects. Taking a look at PPS version 1.0 first (Figure 5a), along most coast in the southern and central portion there is good agreement with mostly neutral or slightly negative differences. However, in the northern part the difference is increasingly positive and very large over Greenland and in regions with a high density of relatively small lakes (e.g. Sweden and Finland). Comparing with corresponding results in Figure 4a it is clear that differences are small but there is at least an indication of slightly more negative differences in the southern and central part of the region.

Over Scandinavia the areas with a lot of lakes consistently show a positive difference of 10-20 % cloud cover. This is present even in the summer month when there is adequate sun light. However, we find the same magnitude of differences also in Figures 4a and 4b so the difference is not remarkable.

For PPS 1.1 there was an interesting change over the northern regions of the domain. Greenland, for example, started showing large negative differences, especially with NOAA 15, indicating a complete switch within PPS resulting in more clouds being reported than MSG – despite the viewing angle effect. Again, this is consistent with the changes seen over the entire region as illustrated in Figure 4b and cannot be assigned specifically to coastal areas.
There were some other changes around the coastal areas of British Isles and northern Norway but these were changes towards smaller differences.

6.9 Cloud Cover Statistics

To complement monthly mean difference results, some overall statistics for cloud cover comparison were collected for NOAA 15 and 17 and it is presented in Tables 1 and 2 below. The statistics is divided into day, night, and twilight conditions using the sun zenith angle. This is based on the same method used by the PPS to determine the sun angle and thus light

conditions. Within these three main categories are sub-categories for land, water, and coastal areas. Under each of these secondary divisions, the following categories were examined along with some permutations: cloudy (including both cloud-filled and cloud contaminated categories) and clear conditions. Cloud contaminated pixels were re-categorized as cloudy pixels.

Table 1: ***Cloud cover statistics for NOAA 15 compared with MSG results for the respective cloud mask products. The red values in brackets represent results from PPS version 1.1 but only for April 2006.***

NOAA15		Day [%]	Night [%]	Twilight [%]
Common pixels	Clear	22.67 (16)	25.67 (41)	28.25 (18)
	Cloudy	61.67 (63)	58.00 (41)	54.75 (62)
MSG Clear PPS Cloudy		6.33 (6)	7.67 (10)	6.00 (10)
MSG Cloudy PPS Clear		9.0 (15)	8.67 (8)	11.00 (10)
Valid pixels		2.15e+09	1.59e+09	1.58e+09
Separation of land and water				
Land				
Common Pixels	Clear	34.0 (23)	33.00 (47)	39.75 (22)
	Cloudy	47.0 (57)	44.00 (34)	40.75 (55)
MSG Clear PPS Cloudy		6.33 (8)	12.67 (11)	7.75 (15)
MSG Cloudy PPS Clear		12.67 (12)	10.00 (7)	11.50 (8)
Valid pixels		8.20e+08	5.88e+08	6.35e+08
Water				
Common Pixels	Clear	14.0 (12)	21.33 (34)	20.25 (15)
	Cloudy	72.67 (66)	66.67 (48)	65.00 (68)
MSG Clear PPS Cloudy		5.67 (4)	4.33 (9)	4.25 (6)
MSG Cloudy PPS Clear		7.0 (17)	8.33 (8)	10.50 (11)
Valid pixels		1.33e+09	1.00e+09	9.48e+08
Coastal Areas: 25 to 75 % Fraction of Land				
Common Pixels	Clear	23.67 (18)	29.67 (31)	29.75 (14)
	Cloudy	56.33 (63)	50.67 (43)	50.50 (64)
MSG Clear PPS Cloudy		9.0 (9)	10.00 (16)	8.50 (15)
MSG Cloudy PPS Clear		11.0 (11)	10.00 (9)	11.25 (7)
Valid pixels		3.52e+08	2.53e+08	2.25e+08
Total number of scenes: 684				

Table 2: ***Same as Table 1 but for NOAA 17 results.***

NOAA17		Day [%]	Night [%]	Twilight [%]
Common pixels	**Clear**	19.0 (19)	26.25 (23)	13.25 (15)
	Cloudy	64.00 (60)	57.75 (57)	61.00 (39)
MSG Clear PPS Cloudy		7.50 (5)	6.75 (7)	2.00 (3)
MSG Cloudy PPS Clear		9.25 (17)	9.25 (14)	23.50 (43)
Valid pixels		2.74e+09	2.90e+09	9.02e+08
Separation of land and water				
Land				
Common Pixels	**Clear**	25.25 (25)	32.25 (32)	26.00 (23)
	Cloudy	51.75 (57)	43 (46)	45.50 (46)
MSG Clear PPS Cloudy		13.00 (7)	10.75 (9)	3.75 (10)
MSG Cloudy PPS Clear		9.75 (11)	10.75 (12)	24.75 (21)
Valid pixels		1.12e+09	1.15e+09	2.59e+08
Water				
Common Pixels	**Clear**	14.75 (14)	20.50 (16)	8.25 (13)
	Cloudy	73.00 (61)	67.25 (64)	67.25 (37)
MSG Clear PPS Cloudy		3.50 (3)	4.25 (5)	1.75 (1)
MSG Cloudy PPS Clear		8.75 (21)	7.75 (15)	23.25 (49)
Valid pixels		1.61e+09	1.75e+09	6.44e+08
Coastal Areas: 25 to 75 % Fraction of Land				
Common Pixels	**Clear**	20.75 (19)	29.00 (21)	24.00 (29)
	Cloudy	61.25 (62)	51.50 (54)	50.00 (40)
MSG Clear PPS Cloudy		6.50 (7)	8.50 (11)	5.00 (7)
MSG Cloudy PPS Clear		11.25 (13)	10.50 (13)	21.50 (24)
Valid pixels		4.00e+08	4.12e+08	1.82e+08
Total number of scenes: 759				

Two tables were constructed showing the statistics of how the two products compared when broken down into the following categories:

- Both clear
- Both cloudy
- One cloudy and the other clear

These four possibilities were examined for day, twilight, night, for coastal areas, over land, and over water. Table 1 shows the results for NOAA 15 for PPS 1.0 with the results for PPS 1.1 (April 2006) in parenthesis. Only April 2006 was reprocessed using PPS 1.1.

For the common cloudy case the percentage of all cases where both products report cloudy for the same pixel ranged from about 40 to 75%, considering different illumination and surface categories. The next category (common clear cases) occurred about 20-40% of the time and varied a few percent between day, night, and twilight. One exception occurred, however, over

water during the day. Here the percentage when both are clear drops to 14%. Thus, we conclude that both MSG and PPS give significantly higher cloud amounts over sea surfaces.

It was also noted that the frequencies of the two difference categories (MSG clear – PPS cloudy and PPS clear – MSG cloudy) are relatively small and normally between 5 and 10%. Possibly there is small tendency for higher values of the second category, i.e., the cloudy category is slightly more frequent for MSG than for PPS. This is probably due to MSG with its high viewing angle picking up more clouds while NOAA looking more nadir more often reports clear. Also, in support of this theory, most of the NOAA satellites scenes were concentrated over the Norwegian Sea and at a high MSG viewing angle. This gives NOAA satellites better spectral resolution than MSG.

For the Coastal areas, the results do not deviate significantly from the land or water categories (as also concluded in the previous section). This indicates that both algorithms treat coastal areas similarly. Nearly all frequencies found here for each category fell between those for the land and water. It would have been interesting to compare results where the cloud masks for both products were created using a specific coastal scheme (an option available at least for the PPS scheme) but the retrieval of such results could unfortunately not be accomplished here. However, since the current study does not find any particular problem or deviation near the coasts we might consider this topic as less important for the moment.

Perhaps the most interesting results are found for NOAA17 in Table 2 for the Twilight category. More specifically, the frequencies for category MSG Cloudy – PPS Clear is generally much higher (even more than twice as high) as for corresponding results for night and daytime and also compared to all corresponding results of NOAA15 in Table 1. For PPS 1.1 results (in brackets in Table 2) the corresponding frequencies even exceed 40 percent. The fact that NOAA 15 results do not show this feature indicates that there might be a problem in the processing of NOAA 17 images. The mentioned difference in the two algorithms where NOAA 15 uses 3.7 μm all the time and NOAA 17 switches between 1.6 μm and 3.7 μm might be a clue to the existence of such differences. To notice is that not all the pixels with twilight flags are processed using NOAA 17's 1.6 μm channel. A mixture between results from 1.6 μm and 3.7 μm is likely to occur during this period. Normally, the switch should occur at the terminator but for practical reasons this cannot be accomplished in a perfect way. In any case, a deeper investigation of the NOAA-17 twilight results is needed to understand the situations.

6.10 Cloud Top Temperature and Height (CTTH)

The results for October 2005 are shown in Figures 6a and 6b with the remaining images for the other months to be found in Appendix A. In each histogram image, the y-axis represents the frequency of heights or temperature (calculated as averages in the 15 km grid) within each respective interval (shown on the x-axis). The max and mean of the MSG values were taken as the basis for establishing which intervals to plot. From these max and min values a set of bins were created. The CTT was created using every 5^{th} degree and the CTH with every ½ km. With each of these intervals or bins, the mean height or temperature was calculated and then the difference (MSG-PPS) was calculated, Due to the low frequencies of occurrences found in some intervals, it may appear that some intervals have no height or temperature values within the top-most and middle plots. This is not the case. It is thus necessary to point out this fact in order to better understand the bottom two difference plots where a difference is shown in intervals that appear to be non zero.

How these cloud heights varied as a function of viewing angle did not reveal anything more than was already seen in figures 5a and b and therefore it was not included in this report.

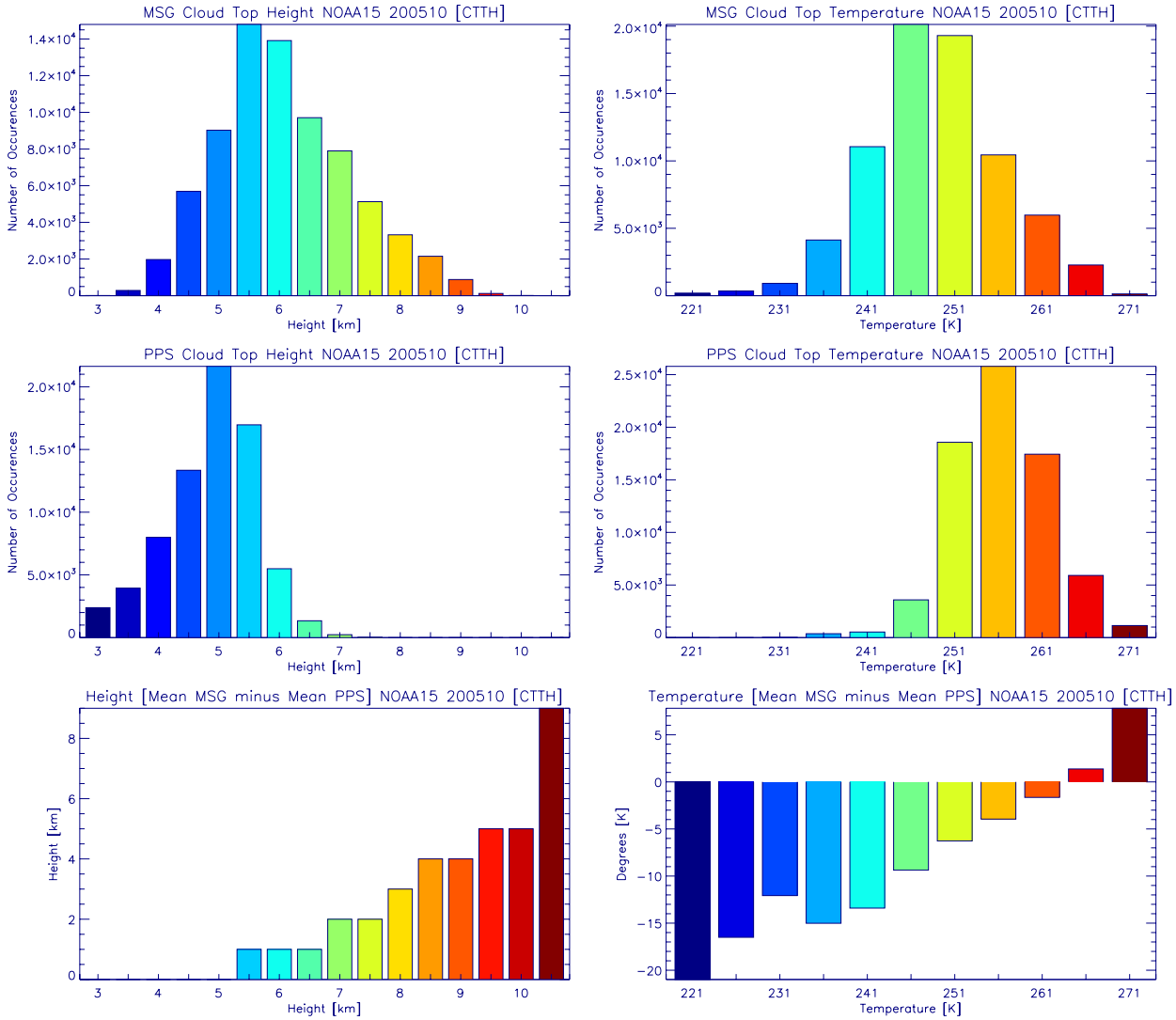

Figure 6a: *The distribution of cloud top temperature and height values. The top two graphs are MSG satellite while the middle two are NOAA. The bottom two graphs show the difference in the difference mean height within each interval. October 2005 for NOAA 15.*

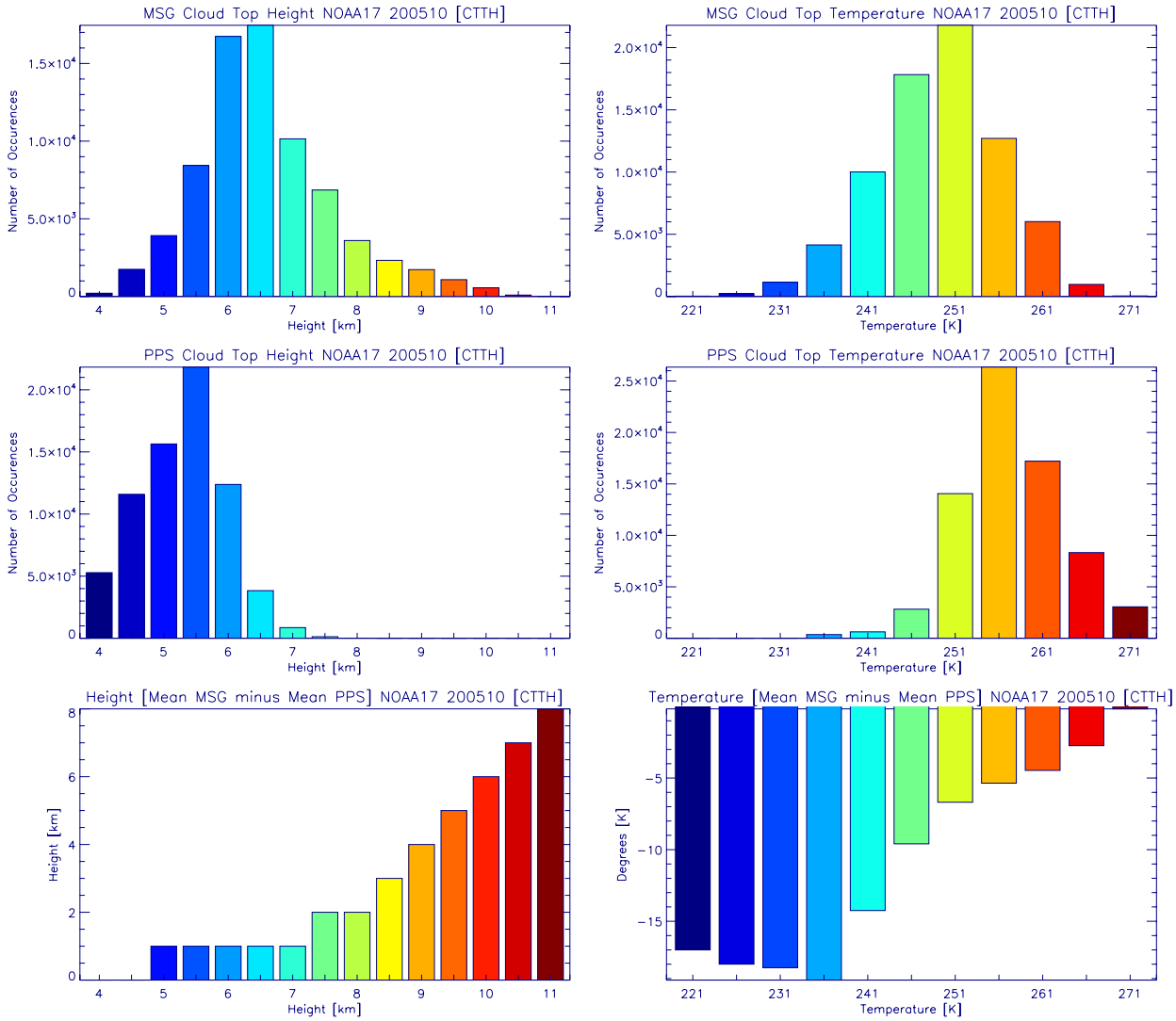

Figure 6b: *The same as figure 6a but for NOAA 17.*

From the results it is very evident that MSG registers a higher frequency of high clouds than both NOAA satellites. The average PPS cloud top lies around 5 km while MSG is around 7 km. In some cases the difference can be more than 4 km. This is consistently seen in the results for all four months and it is reflected in the temperature results as well (i.e., a higher frequency of cold cloud top temperatures for MSG). One curious feature can be seen with both the NOAA satellites during July 2006 (see Figure Ah and Ae in Appendix A). MSG picks up a maximum among the low cloud etage but PPS does not. This maximum appears seasonally consistent (i.e., probably caused by the occurrence of convective Cumulus clouds over land surfaces in summer) but it could be questioned why PPS did not pick up this feature. Further studies are needed here to confirm if this is a serious PPS weakness or not.

7 Conclusions

The goals of this study were to compare the MSG SEVIRI and PPS AVHRR monthly mean cloud products of the CM-SAF. The study was done in two parts: first comparing the cloud mask products and then comparing the cloud top temperature and height products. This was done over a region consisting of twelve CM-SAF tiles and for four seasonally representative months. The region covered the entire European area plus Greenland, parts of

the Arctic Sea in the north, and the most northern part of Africa in the south. Over this area, the PPS data density varied greatly and this variability was quantified.

For the cloud mask using PPS version 1.0, the results showed large problems over the Sahara and parts of Spain during the summer months. This was primarily due to the high reflectances in channel 3a which is similar to clouds reflectances at this wavelength. Since NOAA 17 uses this channel during the day and not NOAA 15, the problem was more prominent in the NOAA 17 results over areas with desert-like conditions.
Much larger differences were found over water than over land surfaces, with the exception of Scandinavia where the differences were comparable to those found over water. The cloud contaminated values were removed in one plot and this revealed that PPS had a larger number of cloud contaminated pixels than MSG. This supports that theory that MSG sees more cloud-filled pixels at higher viewing angles. This also explains why the differences over Scandinavia were so large and positive in value.

The portion of the study that examined the effects of sub-pixel and thin clouds revealed that they affected how well the two products converged. The attempt to use a weighted factor similar that used by (Reuter et. Al. 2007 (submitted)) failed to improve the convergence between the two cloud masks.

The effect of the MSG viewing angle and the subsequent effects of reporting more cloudy pixels (or cloud contaminated pixel – to include thin clouds) could be seen throughout all four months in the form of larger positive divergence at higher latitudes. Problem areas like Greenland remained and varied depending on with polar satellite is being used. It is not yet known why this is so but the low data density certainly played a role. Mountainous areas still pose some problems for both satellites. Figures 5a and b supported this viewing angle theory as it could be clearly seen that MSG reported increased cloudiness as higher and higher viewing angles.
Overall the results showed generally good consistency between satellites and with deviations mainly explained by understandable observation differences (e.g. different viewing angles).

Tables 1 and 2 examined more in detail the differences in the products. The most salient feature is the decrease in agreement between MSG and NOAA 17 for twilight conditions. This is most certainly an effect of how the algorithm handles twilight conditions. Further investigation is needed for this problem

Significant changes were seen when introducing results from the new PPS 1.1 version. A significant decrease in the difference over the Sahara was the most discernable change along with a more reasonable trend for the increasing difference with increasing MSG viewing angle. One exception is the NOAA 17 results from April. Table 2 showed a troubling result during twilight. The cloudy category dropped by nearly half on a whole but mainly over water. This indicates a problem that should be examined more in detail in the future. In addition, the coastal areas, Greenland in particular, saw large swings in the divergence pattern with some switching from positive to negative with the same magnitude. NOAA 15 was mostly affected in this manner than NOAA 17.
The cloud top height and temperature portion of the study supported the earlier results from the cloud mask and revealed even more. In figures 6a and b it is clear that MSG report more higher clouds than PPS. In figures 6a and b it is clear that MSG report more higher clouds than PPS. Furthermore, MSG reported more low clouds during the summer months than PPS which was mostly like due to the presence of convective clouds and the angle at which they

are viewed (small cumulus clouds when viewed from nadir has a smaller diameter than when viewed slantwise). This would make them more detectable by MSG than PPS.

Much more can be done in future studies to include investigation of the cloud type products and PPS version 2.0.

8 Acknowledgment

The authors of the report would like to extend their thanks and appreciation for help rendered during this course of this study. The CM-SAF group at the DWD was very helpful in creating a viable means of data retrieval and data transfer. It was also necessary to re-project the MSG products from satellite projection onto the PPS sinusoidal projection. This was done with the help of Adam Dybbroe which was vital to the success of this study. In addition, special thanks to Ronald Scheirer whose assistance in IDL, among other things, proved extremely helpful.

9 Reference

SAF on Climate Monitoring Science Plan Doc. No. SAF/CM/DWD/SCI/3.3
Issue: 3.3. Date 02-October-2001.

NOAA level 1b Notices: http://www.osdpd.noaa.gov/PSB/PPP/notices/notices.html

Derrien, M., Farki, B., Harang, L., Gléau, H. L., Noyalet, A., Pochic, D., and Sairouni, A., 1993. Automatic cloud detection applied to NOAA-11/AVHRR imagery. *Remote Sensing of Environment 46*, 246.267.

Derrien, M., Lavanant, L., and Gleau, H. L., 1988. Retrieval of the cloud top temperature of semi-transparent clouds with AVHRR. In *Proceedings of the IRS'88, Lille, France*, pp. 199.202.

Derrien M. and H. LeGléau, 2005: MSG/SEVIRI cloud mask and type from SAFNWC, *Int. J. Rem. Sens.*, **26**, 470–4732.

Karlsson, K.-G., 1989. Development of an operational cloud classi_cation model. *International Journal of Remote Sensing 10*, 687.693.

Karlsson, K.-G. and Liljas, E., 1990. The SMHI model for cloud and precipitation analysis from multispectral AVHRR data. PROMIS reports 10, SMHI. 74pp.

Karlsson, K.-G., 1996. Cloud Classi_cation with the SCANDIA model. Reports Meteorology and Climatology 67, SMHI.

Majewski D., D. Liermann, P. Prohl, B. Ritter, M. Buchhold, T. Hanisch, G. Paul, W. Wergen, and J. Baumgardner, 2002: The operational global icosahedral-hexagonal grid point model GME: Description and high resolution tests, *Mon. Wea. Rev.*, **130**, 319-338.

Menzel W.P., W.L. Smith, and T. R. Stewart, 1983: Improved cloud motion wind vector and altitude assignment using VAS. *J. Clim. Appl. Meteor.*, **22**, 377-384.

Saunders, R. and Kriebel, T., 1988. An improved method for detecting clear sky and cloudy radiances from AVHRR data. *Int. J. Rem. Sens. 9*, 123.150.

Stowe, L. L., Davis, P. A., and McClain, E. P., 1999. Scienti_c Basis and Initial Evaluation of the CLAVR-1 Global Clear/Cloud Classi_cation Algorithm for the Advanced Very High Resolution Radiometer. *Journal of Atmospheric and Oceanic Technology 16*, 656.681.

Rueter M, W. Thomas, R. Weber, P. Albert, K-G Karlsson, J. Fischer, 2007, Validation of MSG/SEVIRI-based cloud fractional cover results. (submitted)

Appendix A

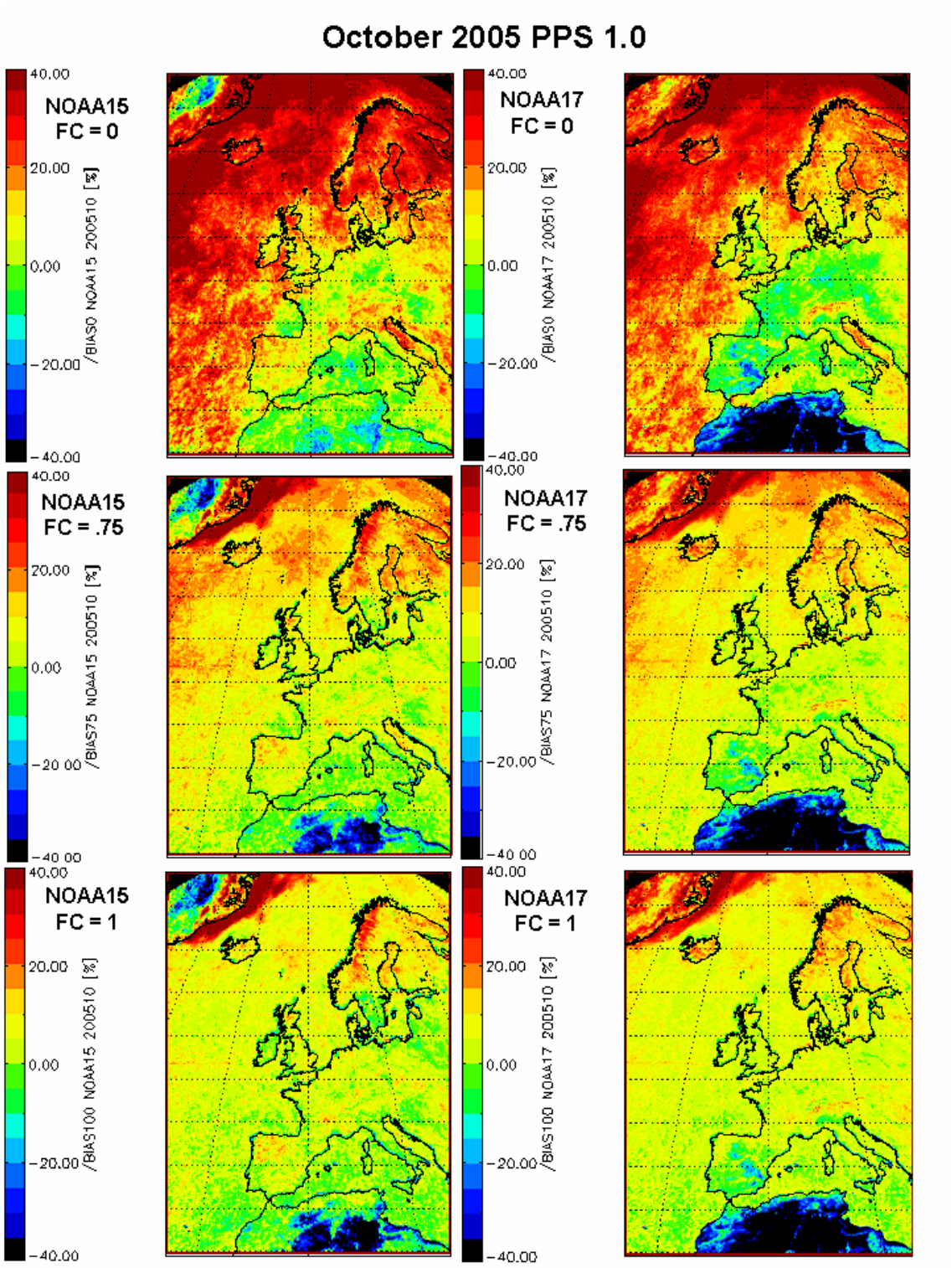

Figure Aa: *The CFC difference: MSG (version 1.2) cloudiness (%) minus PPS (version 1.0) cloudiness (%). NOAA15 (left) and NOAA 17 (right) and a weighting factor for sub-pixel clouds set to 0% (top), 75% (middle), and 100% (bottom). The month was October 2005.*

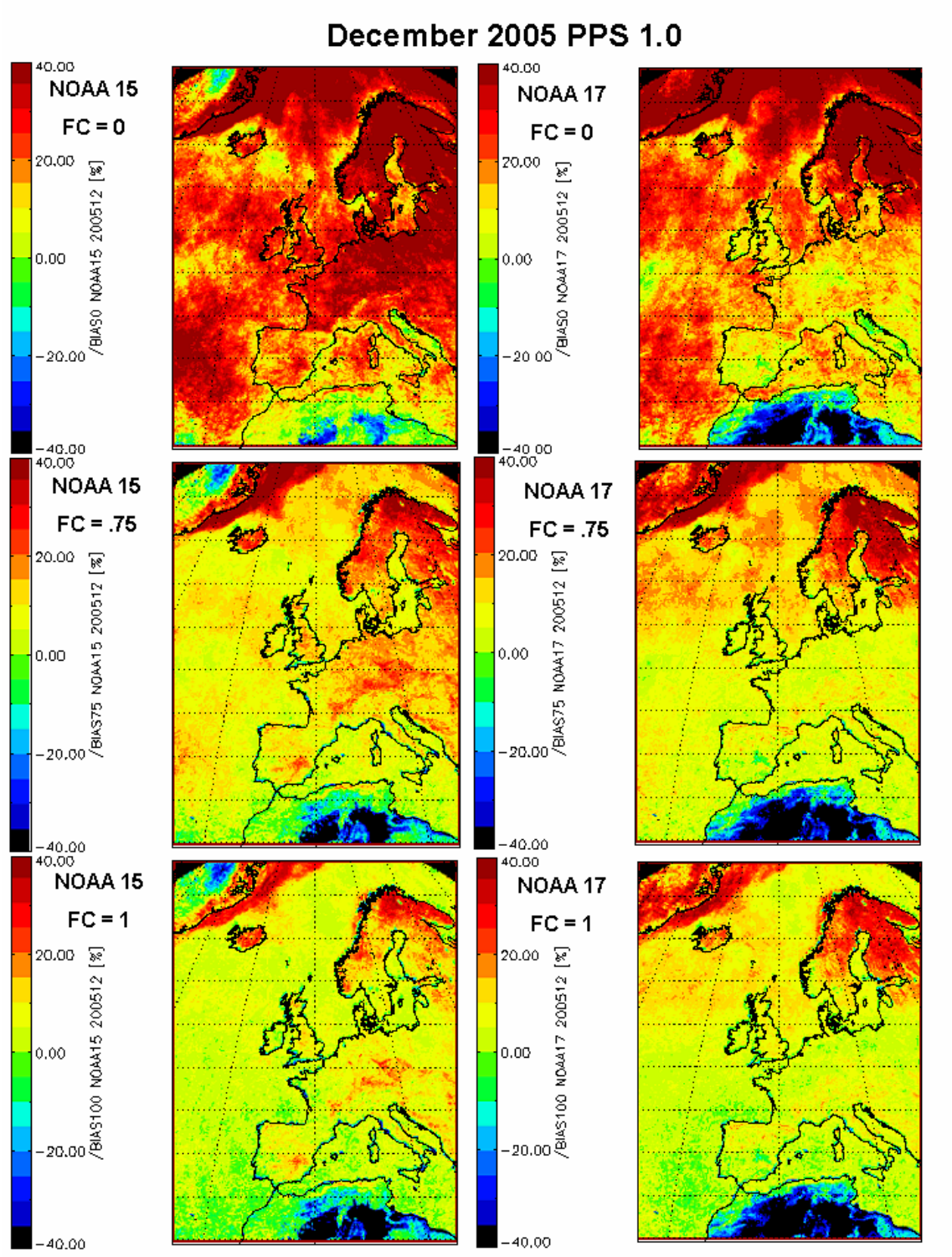

Figure Ab: Same as Ab. *The month was December 2005.*

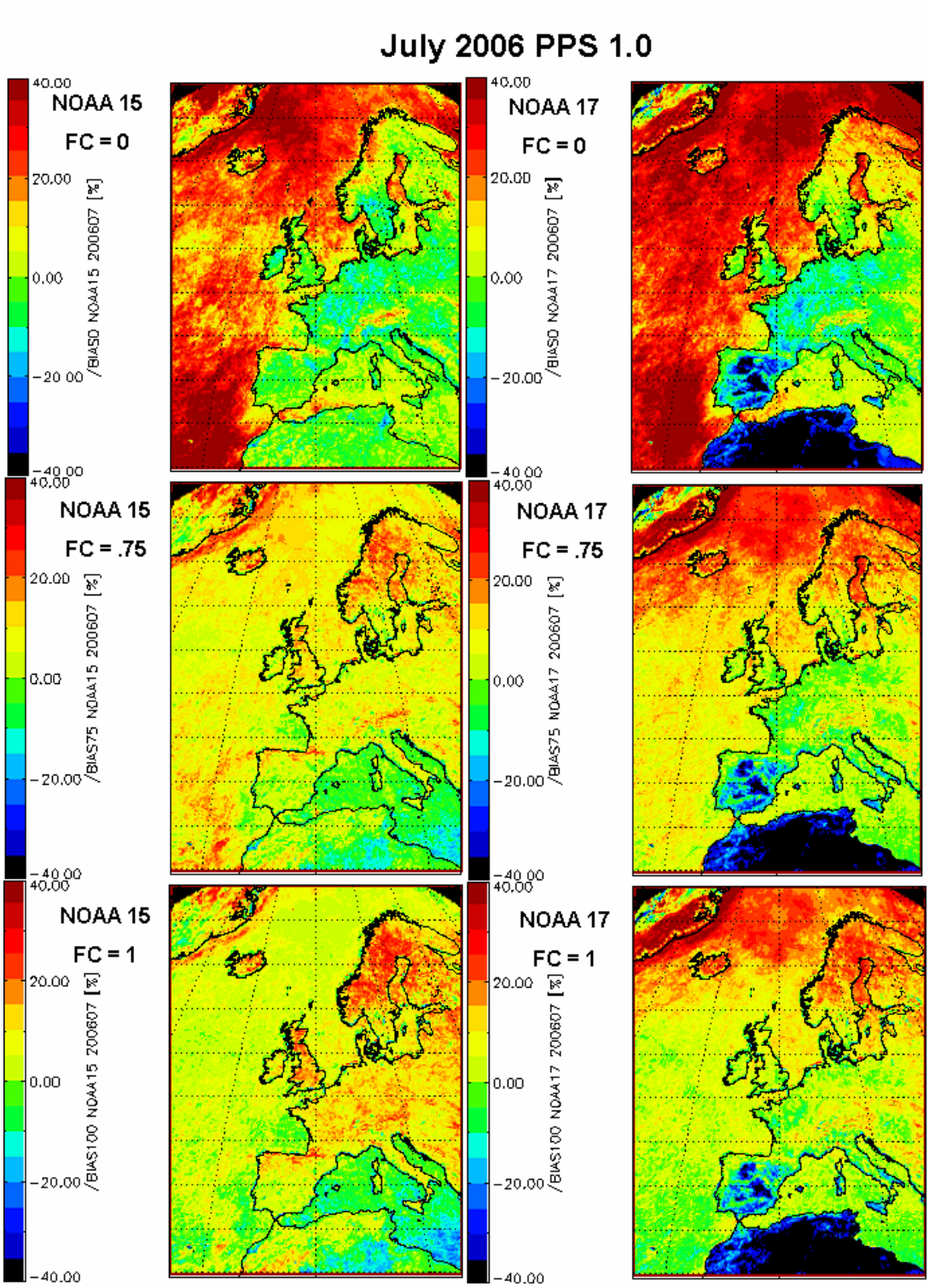

Figure Ac: Same as Aa. The month was July 2006.

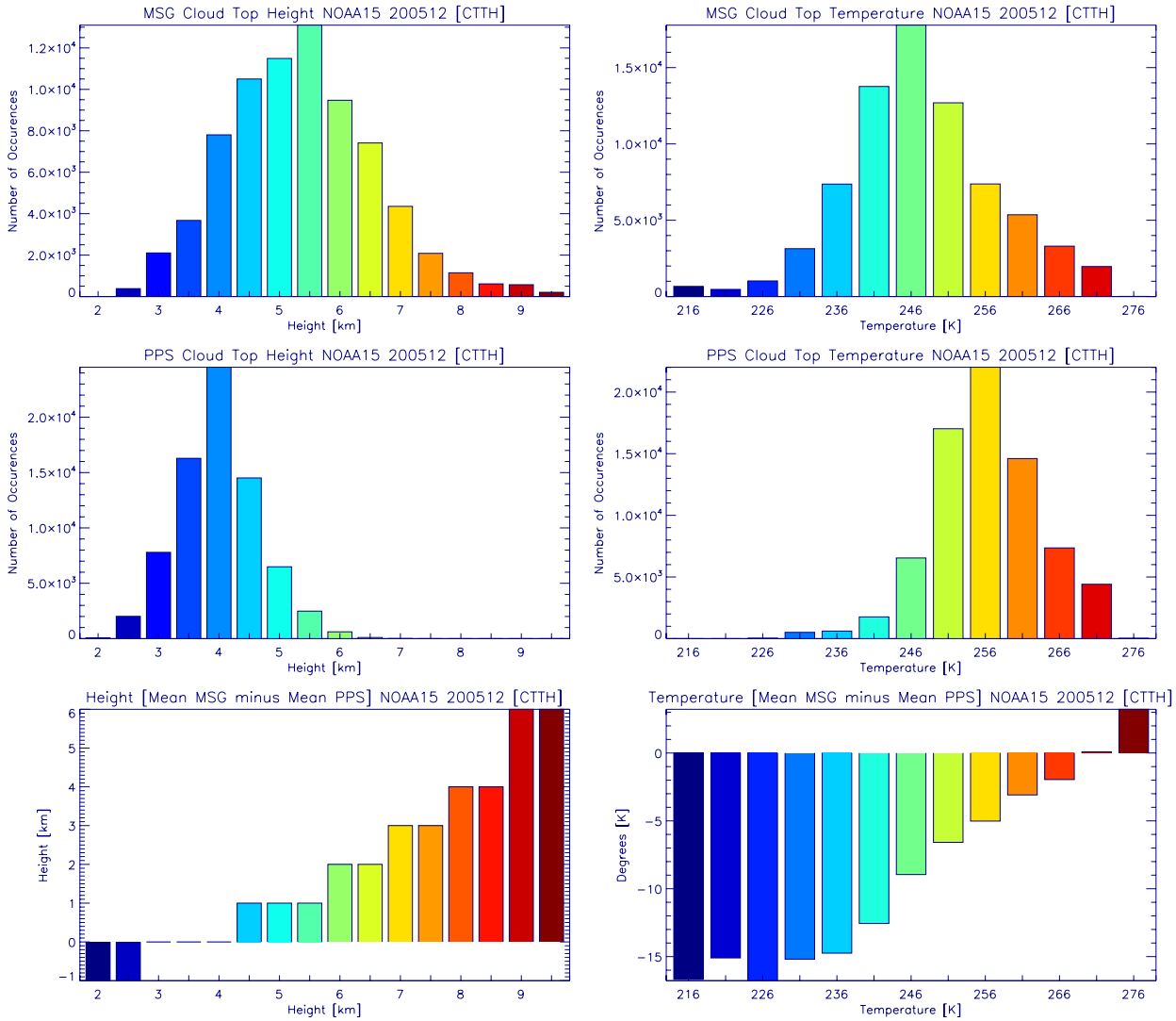

Figure Ad: *shows how the valid pixels from the cloud top temperature and height product are distributed. Top two graphs are from the MSG satellite while the middle two are from PPS. The bottom two graphs show the difference. The date is December 2005 for NOAA 15.*

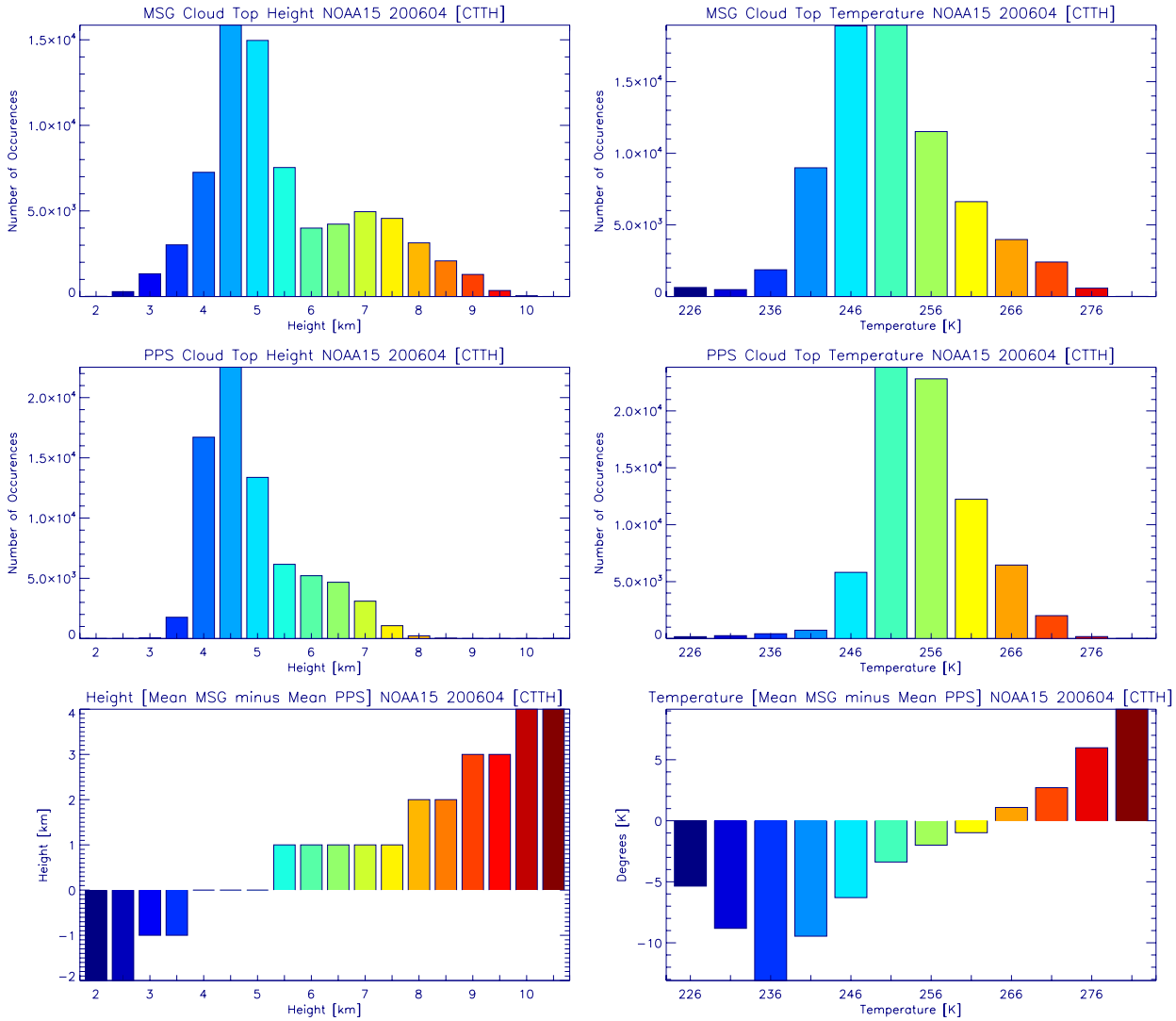

Figure Ad: Same as Ad. *The date is April 2006 for NOAA 15.*

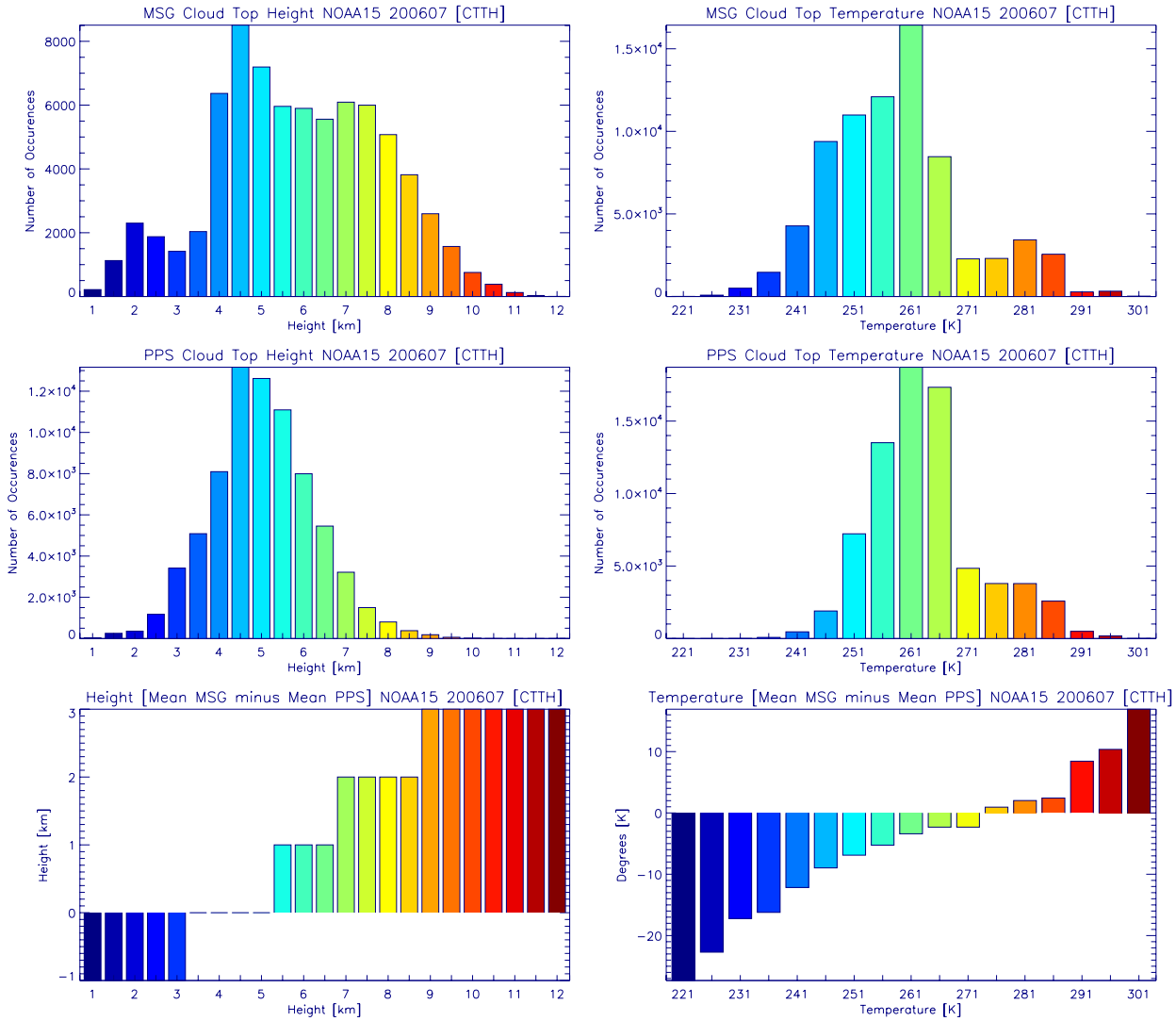

Figure Ae: Same as Ad. *The date is July 2006 for NOAA 15.*

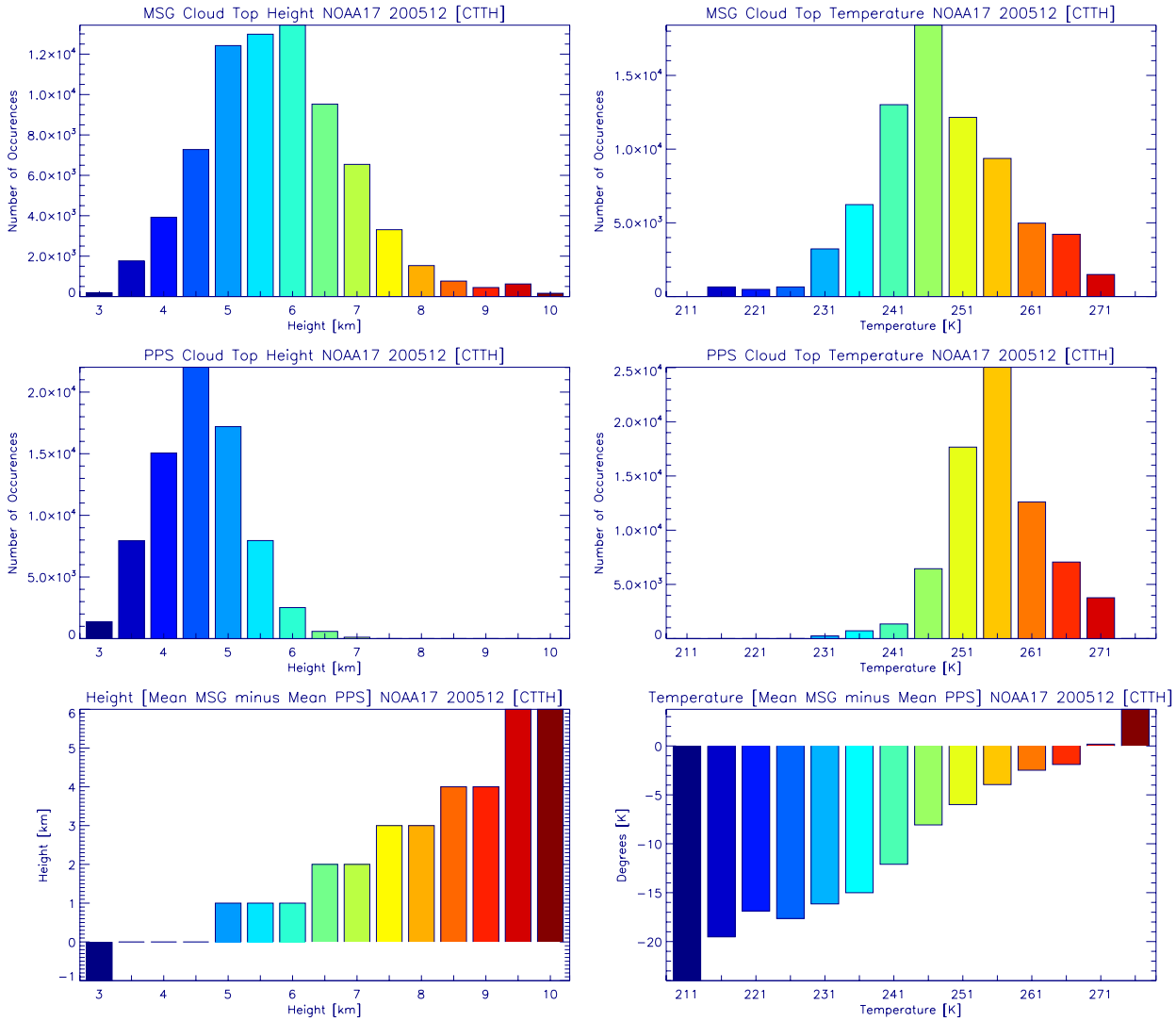

Figure Af: Same as Ad. *The date is December 2005 for NOAA 17.*

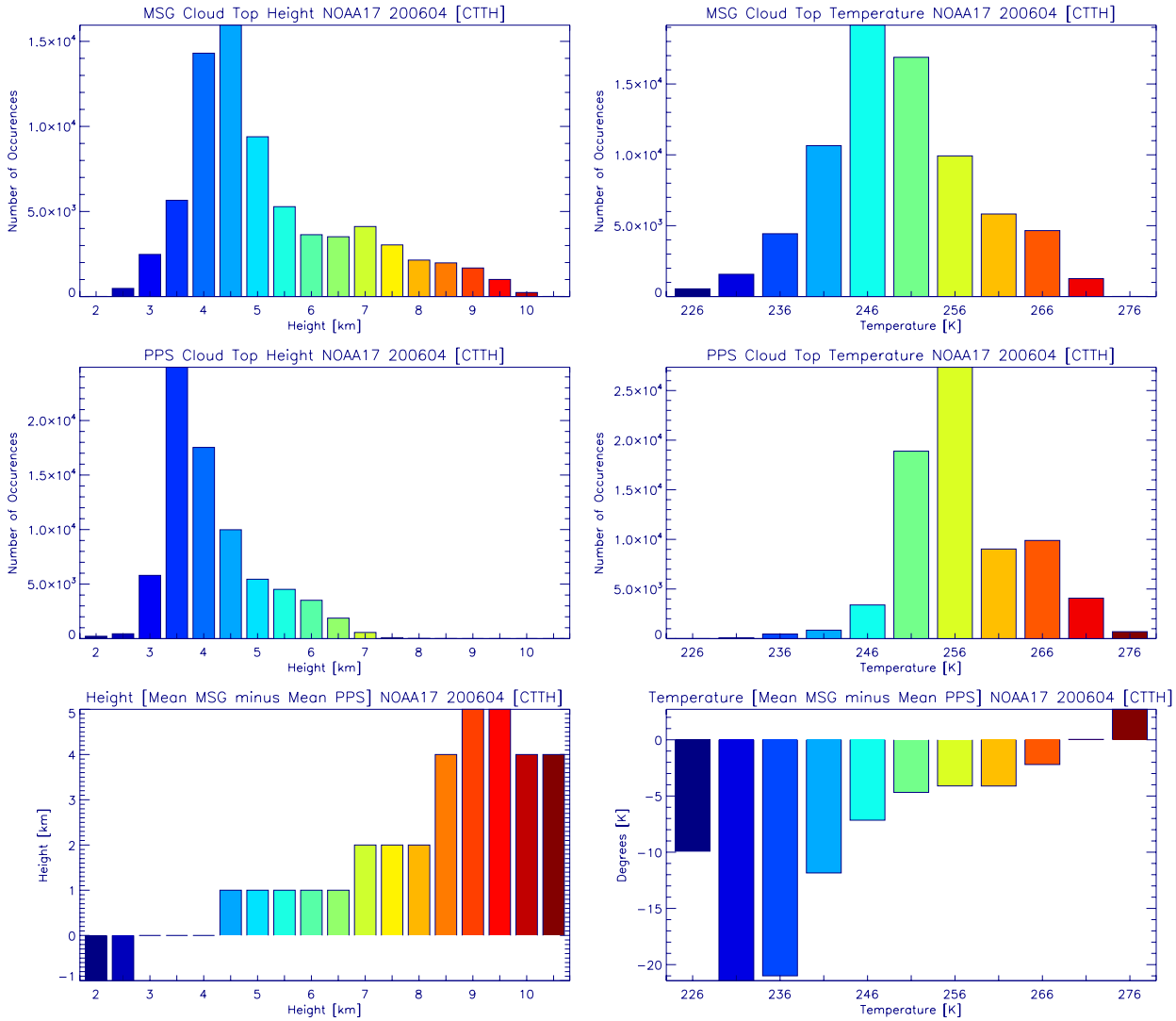

Figure Ag: *Same as Ad. The date is April 2006 for NOAA 17.*

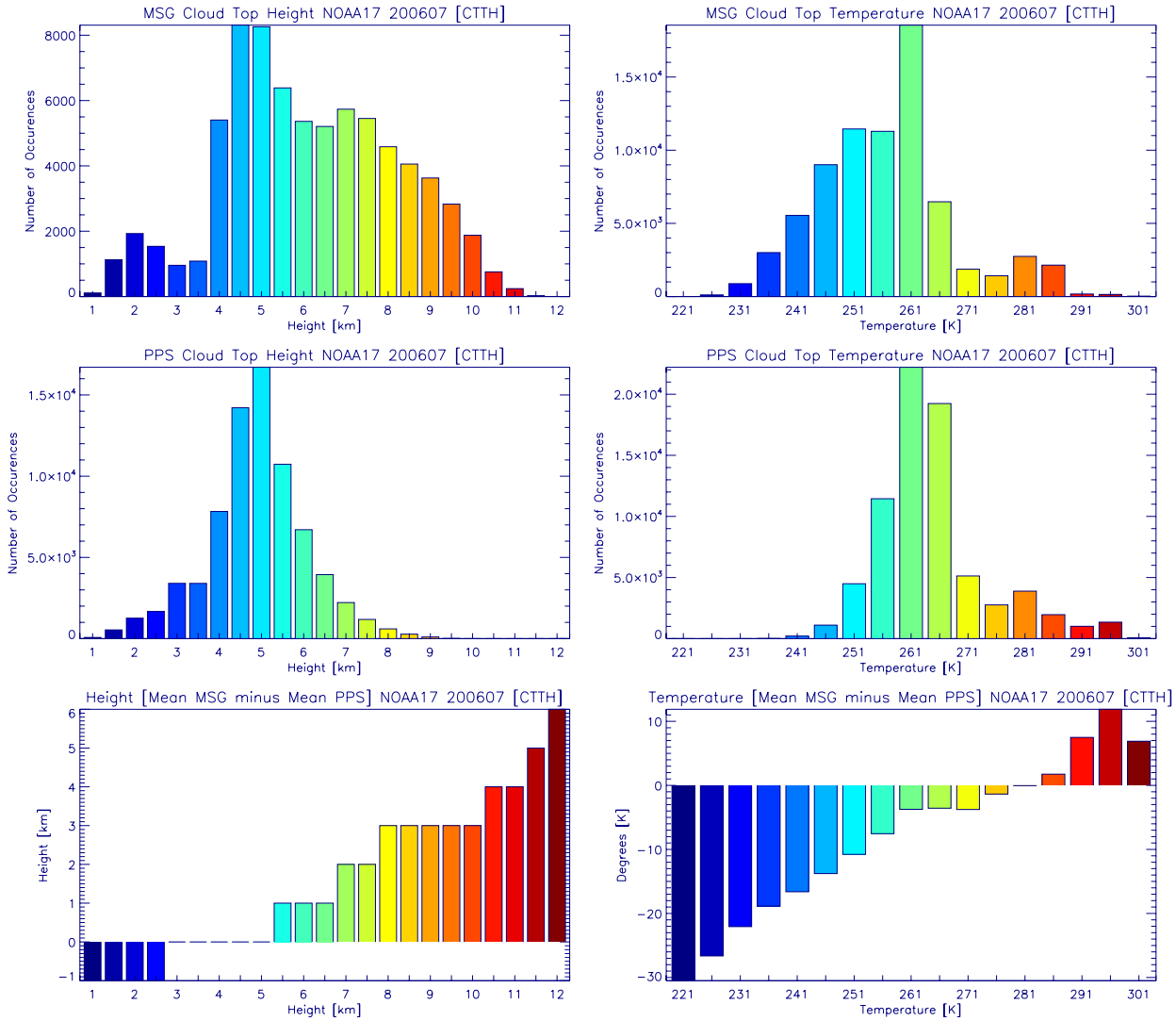

Figure Ah: Same as Ad.. *The date is July 2006 for NOAA 17.*

SMHIs publiceringar

SMHI ger ut sex rapportserier. Tre av dessa, R-serierna är avsedda för internationell publik och skrivs därför oftast på engelska. I de övriga serierna används det svenska språket.

Seriernas namn	**Publiceras sedan**
RMK (Rapport Meteorologi och Klimatologi)	1974
RH (Rapport Hydrologi)	1990
RO (Rapport Oceanografi)	1986
METEOROLOGI	1985
HYDROLOGI	1985
OCEANOGRAFI	1985

I serien METEOROLOGI har tidigare utgivits:

1985

1 Hagmarker, A. (1985)
Satellitmeteorologi.

2 Fredriksson, U., Persson, Ch., Laurin, S. (1985)
Helsingborgsluft.

3 Persson, Ch., Wern, L. (1985)
Spridnings- och depositionsberäkningar för av fallsförbränningsanläggningar i Sofielund och Högdalen.

4 Kindell, S. (1985)
Spridningsberäkningar för SUPRAs anläggningar i Köping.

5 Andersson, C., Kvick, T. (1985)
Vindmätningar på tre platser på Gotland. Utvärdering nr 1.

6 Kindell, S. (1985)
Spridningsberäkningar för Ericsson, Ingelstafabriken.

7 Fredriksson, U. (1985)
Spridningsberäkningar för olika plymlyft vid avfallsvärmeverket Sävenäs.

8 Fredriksson, U., Persson, Ch. (1985)
NO_x- och NO_2-beräkningar vid Vasaterminalen i Stockholm.

9 Wern, L. (1985)
Spridningsberäkningar för ASEA transformers i Ludvika.

10 Axelsson, G., Eklind, R. (1985)
Ovädret på Östersjön 23 juli 1985.

11 Laurin, S., Bringfelt, B. (1985)
Spridningsmodell för kväveoxider i gatumiljö.

12 Persson, Ch., Wern, L. (1985)
Spridnings- och depositionsberäkningar för avfallsförbränningsanläggning i Sofielund.

13 Persson, Ch., Wern, L. (1985)
Spridnings- och depositionsberäkningar för avfallsförbränningsanläggning i Högdalen.

14 Vedin, H., Andersson, C. (1985)
Extrema köldperioder i Stockholm.

15 Krieg, R., Omstedt, G. (1985)
Spridningsberäkningar för Volvos planerade bilfabrik i Uddevalla.

16 Kindell, S. Wern, L. (1985)
Luftvårdsstudie avseende industrikombinatet i Nynäshamn (koncentrations- och luktberäkningar).

17 Laurin, S., Persson, Ch. (1985)
Beräknad formaldehydspridning och deposition från SWEDSPANs spånskivefabrik.

18 Persson, Ch., Wern, L. (1985)
Luftvårdsstudie avseende industri-kombinatet i Nynäshamn – depositions-beräkningar av koldamm.

19 Fredriksson, U. (1985)
Luktberäkningar för Bofors Plast i Ljungby, II.

20 Wern, L., Omstedt, G. (1985)
Spridningsberäkningar för Volvos planerade bilfabrik i Uddevalla - energicentralen.

21 Krieg, R., Omstedt, G. (1985)
Spridningsberäkningar för Volvos planerade bilfabrik i Uddevalla - kompletterande beräkningar för fabrikerna.

22 Karlsson, K.-G. (1985)
Information från Meteosat - forskningsrön och operationell tillämpning.

23 Fredriksson, U. (1985)
Spridningsberäkningar för AB Åkerlund & Rausings fabrik i Lund.

24 Färnlöf, S. (1985)
Radarmeteorologi.

25 Ahlström, B., Salomonsson, G. (1985)
Resultat av 5-dygnsprognos till ledning för isbrytarverksamhet vintern 1984-85.

26 Wern, L. (1985)
Avesta stadsmodell.

27 Hultberg, H. (1985)
Statistisk prognos av yttemperatur.

1986

1 Krieg, R., Johansson, L., Andersson, C. (1986)
Vindmätningar i höga master, kvartalsrapport 3/1985.

2 Olsson, L.-E., Kindell, S. (1986)
Air pollution impact assessment for the SABAH timber, pulp and paper complex.

3 Ivarsson, K.-I. (1986)
Resultat av byggväderprognoser - säsongen 1984/85.

4 Persson, Ch., Robertson, L. (1986)
Spridnings- och depositionsberäkningar för en sopförbränningsanläggning i Skövde.

5 Laurin, S. (1986)
Bilavgaser vid intagsplan - Eskilstuna.

6 Robertson, L. (1986)
Koncentrations- och depositionsberäkningar för en sopförbränningsanläggning vid Ryaverken i Borås.

7 Laurin, S. (1986)
Luften i Avesta - föroreningsbidrag från trafiken.

8 Robertson, L., Ring, S. (1986)
Spridningsberäkningar för bromcyan.

9 Wern, L. (1986)
Extrema byvindar i Orrefors.

10 Robertson, L. (1986)
Koncentrations- och depositionsberäkningar för Halmstads avfallsförbränningsanläggning vid Kristinehed.

11 Törnevik, H., Ugnell (1986)
Belastningsprognoser.

12 Joelsson, R. (1986)
Något om användningen av numeriska prognoser på SMHI (i princip rapporten till ECMWF).

13 Krieg, R., Andersson, C. (1986)
Vindmätningar i höga master, kvartalsrapport 4/1985.

14 Dahlgren, L. (1986)
Solmätning vid SMHI.

15 Wern, L. (1986)
Spridningsberäkningar för ett kraftvärmeverk i Sundbyberg.

16 Kindell, S. (1986)
Spridningsberäkningar för Uddevallas fjärrvärmecentral i Hovhult.

17 Häggkvist, K., Persson, Ch., Robertson, L (1986)
Spridningsberäkningar rörande gasutsläpp från ett antal källor inom SSAB Luleåverken.

18 Krieg, R., Wern, L. (1986)
En klimatstudie för Arlanda stad.

19 Vedin, H. (1986)
Extrem arealnederbörd i Sverige.

20 Wern, L. (1986)
Spridningsberäkningar för lösningsmedel i Tibro.

21 Krieg, R., Andersson, C. (1986)
Vindmätningar i höga master - kvartalsrapport 1/1986.

22 Kvick, T. (1986)
Beräkning av vindenergitillgången på några platser i Halland och Bohuslän.

23 Krieg, R., Andersson, C. (1986)
Vindmätningar i höga master - kvartalsrapport 2/1986.

24 Persson, Ch. (SMHI), Rodhe, H. (MISU), De Geer, L.-E. (FOA) (1986)
Tjernobylolyckan - En meteorologisk analys av hur radioaktivitet spreds till Sverige.

25 Fredriksson, U. (1986)
Spridningsberäkningar för Spendrups bryggeri, Grängesberg.

26 Krieg, R. (1986)
Beräkningar av vindenergitillgången på några platser i Skåne.

27 Wern, L., Ring, S. (1986)
Spridningsberäkningar, SSAB.

28 Wern, L., Ring, S. (1986)
Spridningsberäkningar för ny ugn, SSAB II.

29 Wern, L. (1986)
Spridningsberäkningar för Volvo Hallsbergverken.

30 Fredriksson, U. (1986)
SO_2-halter från Hammarbyverket kring ny arena vid Johanneshov.

31 Persson, Ch., Robertson, L., Häggkvist, K. (1986)
Spridningsberäkningar, SSAB - Luleåverken.

32 Kindell, S., Ring, S. (1986)
Spridningsberäkningar för SAABs planerade bilfabrik i Malmö.

33 Wern, L. (1986)
Spridningsberäkningar för svavelsyrafabrik i Falun.

34 Wern, L., Ring, S. (1986)
Spridningsberäkningar för Västhamnsverket HKV1 i Helsingborg.

35 Persson, Ch., Wern, L. (1986)
Beräkningar av svaveldepositionen i Stockholmsområdet.

36 Joelsson, R. (1986)
USAs månadsprognoser.

37 Vakant nr.

38 Krieg, R., Andersson, C. (1986)
Utemiljön vid Kvarnberget, Lysekil.

39 Häggkvist, K. (1986)
Spridningsberäkningar av freon 22 från Ropstens värmepumpverk.

40 Fredriksson, U. (1986)
Vindklassificering av en plats på Hemsön.

41 Nilsson, S. (1986)
Utvärdering av sommarens (1986) använda konvektionsprognoshjälpmedel.

42 Krieg, R., Kvick, T. (1986)
Vindmätningar i höga master.

43 Krieg, R., Fredriksson, U. (1986)
Vindarna över Sverige.

44 Robertson, L. (1986)
Spridningsberäkningar rörande gasutsläpp vid ScanDust i Landskrona - bestämning av cyanvätehalter.

45 Kvick, T., Krieg, R., Robertson, L. (1986)
Vindförhållandena i Sveriges kust- och havsband, rapport nr 2.

46 Fredriksson, U. (1986)
Spridningsberäkningar för en planerad panncentral vid Lindsdal utanför Kalmar.

47 Fredriksson, U. (1986)
Spridningsberäkningar för Volvo BMs fabrik i Landskrona.

48 Fredriksson, U. (1986)
Spridningsberäkningar för ELMO-CALFs fabrik i Svenljunga.

49 Häggkvist, K. (1986)
Spridningsberäkningar rörande gasutsläpp från syrgas- och bensenupplag inom SSAB Luleåverken.

50 Wern, L., Fredriksson, U., Ring, S. (1986)
Spridningsberäkningar för lösningsmedel i Tidaholm.

51 Wern, L. (1986)
Spridningsberäkningar för Volvo BM ABs anläggning i Braås.

52 Ericson, K. (1986)
Meteorological measurements performed May 15, 1984, to June, 1984, by the SMHI.

53 Wern, L., Fredriksson, U. (1986)
Spridningsberäkning för Kockums Plåtteknik, Ronneby.

54 Eriksson, B. (1986)
Frekvensanalys av timvisa temperaturobservationer.

55 Wern, L., Kindell, S. (1986)
Luktberäkningar för AB ELMO i Flen.

56 Robertson, L. (1986)
Spridningsberäkningar rörande utsläpp av NO_x inom Fagersta kommun.

57 Kindell, S. (1987)
Luften i Nässjö.

58 Persson, Ch., Robertson, L. (1987)
Spridningsberäkningar rörande gasutsläpp vid ScanDust i Landskrona - bestämning av cyanväte.

59 Bringfelt, B. (1987)
Receptorbaserad partikelmodell för gatumiljömodell för en gata i Nyköping.

60 Robertson, L. (1987)
Spridningsberäkningar för Varbergs kommun. Bestämning av halter av SO_2, CO, NO_x samt några kolväten.

61 Vedin, H., Andersson, C. (1987)
E 66 - Linderödsåsen - klimatförhållanden.

62 Wern, L., Fredriksson, U. (1987)
Spridningsberäkningar för Kockums Plåtteknik, Ronneby. 2.

63 Taesler, R., Andersson, C., Wallentin, C., Krieg, R. (1987)
Klimatkorrigering för energiförbrukningen i ett eluppvärmt villaområde.

64 Fredriksson, U. (1987)
Spridningsberäkningar för AB Åetå-Trycks planerade anläggning vid Kungens Kurva.

65 Melgarejo, J. (1987)
Mesoskalig modellering vid SMHI.

66 Häggkvist, K. (1987)
Vindlaster på kordahus vid Alviks Strand - numeriska beräkningar.

67 Persson, Ch. (1987)
Beräkning av lukt och föroreningshalter i luft runt Neste Polyester i Nol.

68 Fredriksson, U., Krieg, R. (1987)
En överskalig klimatstudie för Tornby, Linköping.

69 Häggkvist, K. (1987)
En numerisk modell för beräkning av vertikal momentumtransport i områden med stora råhetselement. Tillämpning på ett energiskogsområde.

70 Lindström, Kjell (1987)
Weather and flying briefing aspects.

71 Häggkvist, K. (1987)
En numerisk modell för beräkning av vertikal momentumtransport i områden med stora råhetselement. En koefficientbestämning.

72 Liljas, E. (1988)
Förbättrad väderinformation i jordbruket - behov och möjligheter (PROFARM).

73 Andersson, Tage (1988)
Isbildning på flygplan.

74 Andersson, Tage (1988)
Aeronautic wind shear and turbulence.
A review for forecasts.

75 Källberg, P. (1988)
Parameterisering av diabatiska processer i numeriska prognosmodeller.

76 Vedin, H., Eriksson, B. (1988)
Extrem arealnederbörd i Sverige 1881 - 1988.

77 Eriksson, B., Carlsson, B., Dahlström, B. (1989)
Preliminär handledning för korrektion av nederbördsmängder.

78 Liljas, E. (1989)
Torv-väder. Behovsanalys med avseende på väderprognoser och produktion av bränsletorv.

79 Hagmarker, A. (1991)
Satellitmeteorologi.

80 Lövblad, G., Persson, Ch. (1991)
Background report on air pollution situation in the Baltic states - a prefeasibility study.
IVL Publikation B 1038.

81 Alexandersson, H., Karlström, C., Larsson-McCann, S. (1991)
Temperaturen och nederbörden i Sverige 1961-90. Referensnormaler.

82 Vedin, H., Alexandersson, H., Persson, M. (1991)
Utnyttjande av persistens i temperatur och nederbörd för vårflödesprognoser.

83 Moberg, A. (1992)
Lufttemperaturen i Stockholm 1756 - 1990. Historik, inhomogeniteter och urbaniseringseffekt.
Naturgeografiska Institutionen, Stockholms Universitet.

84 Josefsson, W. (1993)
Normalvärden för perioden 1961-90 av globalstrålning och solskenstid i Sverige.

85 Laurin, S., Alexandersson, H. (1994)
Några huvuddrag i det svenska temperatur-klimatet 1961 - 1990.

86 Fredriksson, U. och Ståhl, S. (1994)
En jämförelse mellan automatiska och manuella fältmätningar av temperatur och nederbörd.

87 Alexandersson, H., Eggertsson Karlström, C. och Laurin S. (1997).
Några huvuddrag i det svenska nederbördsklimatet 1961-1990.

88 Mattsson, J., Rummukainen, M. (1998)
Växthuseffekten och klimatet i Norden - en översikt.

89 Kindbom, K., Sjöberg, K., Munthe, J., Peterson, K. (IVL)
Persson, C. Roos, E., Bergström, R. (SMHI). (1998)
Nationell miljöövervakning av luft- och nederbördskemi 1996.

90 Foltescu, V.L., Häggmark, L (1998)
Jämförelse mellan observationer och fält med griddad klimatologisk information.

91 Hultgren, P., Dybbroe, A., Karlsson, K.-G. (1999)
SCANDIA – its accuracy in classifying LOW CLOUDS

92 Hyvarinen, O., Karlsson, K.-G., Dybbroe, A. (1999)
Investigations of NOAA AVHRR/3 1.6 μm imagery for snow, cloud and sunglint discrimination
(Nowcasting SAF)

93 Bennartz, R., Thoss, A., Dybbroe, A. and Michelson, D. B. (1999)
Precipitation Analysis from AMSU
(Nowcasting SAF)

94 Appelqvist, Peter och Anders Karlsson (1999)
Nationell emissionsdatabas för utsläpp till luft - Förstudie.

95 Persson, Ch., Robertson L. (SMHI)
Thaning, L (LFOA). (2000)
Model for Simulation of Air and Ground Contamination Associated with Nuclear Weapons. An Emergency Preparedness Model.

96 Kindbom K., Svensson A., Sjöberg K., (IVL) Persson C., (SMHI) (2001)
Nationell miljöövervakning av luft- och nederbördskemi 1997, 1998 och 1999.

97 Diamandi, A., Dybbroe, A. (2001)
Nowcasting SAF
Validation of AVHRR cloud products.

98 Foltescu V. L., Persson Ch. (2001)
Beräkningar av moln- och dimdeposition i Sverigemodellen - Resultat för 1997 och 1998.

99 Alexandersson, H. och Eggertsson Karlström, C (2001)
Temperaturen och nederbörden i Sverige 1961-1990. Referensnormaler - utgåva 2.

100 Korpela, A., Dybbroe, A., Thoss, A. (2001)
Nowcasting SAF - Retrieving Cloud Top Temperature and Height in Semi-transparent and Fractional Cloudiness using AVHRR.

101 Josefsson, W. (1989)
Computed global radiation using interpolated, gridded cloudiness from the MESA-BETA analysis compared to measured global radiation.

102 Foltescu, V., Gidhagen, L., Omstedt, G. (2001)
Nomogram för uppskattning av halter av PM_{10} och NO_2

103 Omstedt, G., Gidhagen, L., Langner, J. (2002)
Spridning av förbränningsemissioner från småskalig biobränsleeldning
– analys av PM2.5 data från Lycksele med hjälp av två Gaussiska spridningsmodeller.

104 Alexandersson, H. (2002)
Temperatur och nederbörd i Sverige 1860 - 2001

105 Persson, Ch. (2002)
Kvaliteten hos nederbördskemiska mätdata som utnyttjas för dataassimilation i MATCH-Sverige modellen".

106 Mattsson, J., Karlsson, K-G. (2002)
CM-SAF cloud products feasibility study in the inner Arctic region
Part I: Cloud mask studies during the 2001 Oden Arctic expedition

107 Kärner, O., Karlsson, K-G. (2003)
Climate Monitoring SAF - Cloud products feasibility study in the inner Arctic region.
Part II: Evaluation of the variability in radiation and cloud data

108 Persson, Ch., Magnusson, M. (2003)
Kvaliteten i uppmätta nederbördsmängder inom svenska nederbörskemiska stationsnät

109 Omstedt, G., Persson Ch., Skagerström, M (2003)
Vedeldning i småhusområden

110 Alexandersson, H., Vedin, H. (2003)
Dimensionerande regn för mycket små avrinningsområden

111 Alexandersson, H. (2003)
Korrektion av nederbörd enligt enkel klimatologisk metodik

112 Joro, S., Dybbroe, A.(2004)
Nowcasting SAF – IOP
Validating the AVHRR Cloud Top Temperature and Height product using weather radar data
Visiting Scientist report

113 Persson, Ch., Ressner, E., Klein, T. (2004)
Nationell miljöövervakning – MATCH-Sverige modellen
Metod- och resultatsammanställning för åren 1999-2002 samt diskussion av osäkerheter, trender och miljömål

114 Josefsson, W. (2004)
UV-radiation measured in Norrköping 1983-2003.

115 Martin, Judit, (2004)
Var tredje timme – Livet som väderobservatör

116 Gidhagen, L., Johansson, C., Törnquist, L. (2004)
NORDIC – A database for evaluation of dispersion models on the local, urban and regional scale

117 Langner, J., Bergström, R., Klein, T., Skagerström, M. (2004)
Nuläge och scenarier för inverkan på marknära ozon av emissioner från Västra Götalands län – Beräkningar för 1999

118 Trolez, M., Tetzlaff, A., Karlsson, K-G. (2005)
CM-SAF Validating the Cloud Top Height product using LIDAR data

119 Rummukainen, M. (2005)
Växthuseffekten

120 Omstedt, G. (2006)
Utvärdering av PM_{10} - mätningar i några olika nordiska trafikmiljöer

121 Alexandersson, H. (2006)
Vindstatistik för Sverige 1961-2004

122 Samuelsson, P., Gollvik, S., Ullerstig, A., (2006)
The land-surface scheme of the Rossby Centre regional atmospheric climate model (RCA3)

123 Omstedt, G. (2007)
VEDAIR – ett internetverktyg för beräkning av luftkvalitet vid småskalig biobränsleeldning
Modellbeskrivning och slutrapport mars 2007

124 Persson, G., Strandberg, G., Bärring, L., Kjellström, E. (2007)
Beräknade temperaturförhållanden för tre platser i Sverige – perioderna 1961-1990 och 2011-2040

125 Engart, M., Foltescu, V. (2007)
Luftföroreningar i Europa under framtida klimat

126 Jansson, A., Josefsson, W
Modelling of surface global radiation and CIE-weighted UV-radiation for the period 1980-2000

Sveriges meteorologiska och hydrologiska institut
601 76 Norrköping · Tel 011-495 8000 · Fax 011-495 8001
www.smhi.se

ISSN 0283-7730